RESOPNE TO REVIEWER2

Thank you very much for taking the time to provide valuable feedback on our manuscript. Your input is highly significant in improving the quality of our manuscript.

To demonstrate our appreciation for your feedback, we have diligently addressed each of your comments and made significant revisions, particularly in the following areas. We rearranged the logic of the manuscript and added data, especially for the xylem water of Qinghai spruce. The water vapor recirculation part is clearly expounded, and each parameter is described in detail. We haved carried out uncertainty analysis.We have re-landscaped all the images throughout the article and improved their clarity.We have changed the language to make it easier for native English speakers to make valuable suggestions.We have placed the revised manuscript PDF at the end of the document. The red bolded words, sentences, and subsections in the manuscript represent our editing changes.

We sincerely hope that you will recognize the genuine effort we have put into this manuscript and give us another opportunity to review and incorporate your suggested modifications.

General comment

The authors of this manuscript aimed to assess the role of transpiration, compared to other water fluxes, in a spruce forest in the Qilian Mountains, China. In their analyses, the authors exploited the usefulness of stable isotopes of hydrogen and oxygen to investigate water fluxes in the soil-plant-atmosphere continuum.

Respone: Thank you for your affirmation of our work. It serves as an ongoing motivation for us to continue our research in the current direction. We greatly appreciate your support and encouragement.

Although this manuscript may be interesting for the readers of Hydrology and Earth System Sciences, the current version presents a poor description of the sampling

approaches and laboratory methodologies, and the dataset does not seem sufficient to support the main findings (only a growing season was considered, and the authors collected only 7 xylem samples). Furthermore, the authors should have determined the uncertainty in their estimates, in order to assess the impacts on the main results.

Respone: This issue indeed serves as a critical weakness in our manuscript. Therefore, in this revised version, we have made several adjustments. Firstly, we have adjusted the research timeframe to cover two growing seasons from 2018 to 2019. Additionally, we have increased the number of sampling points to four at different vertical heights and expanded the number of wood water samples to 404. Furthermore, we have conducted an uncertainty analysis (Section 5.2) to assess the uncertainties associated with our methodology.

In terms of presentation quality, the manuscript would benefit from a thorough revision of the English by a native speaker, and the authors should upload high-resolution figures with labels that are readable.

Respone: To underscore our determination to enhance the quality of the manuscript, we have undertaken a complete revamp of all the visuals in the article. Furthermore, we have made language revisions throughout the manuscript to ensure it is better suited for native English speakers to read and comprehend.

Specific comments

Section 1: I think the introduction lacks some paragraphs describing the usefulness of stable isotopes of hydrogen and oxygen to investigate water fluxes in the soil-plant-atmosphere continuum. Furthermore, the novelty of this work is not clear (it seems a case study, but there are many like this one), and the specific objectives and/or the research questions should be clearly addressed.

Respone: Thank you for your feedback. We have inserted the following sentence into the introduction:

The interaction between soil and vegetation controls rainfall input and water

transfer within ecosystem components. It is an important player in climate change mitigation in terms of climate benefits (Rohatyn et al., 2022). In the face of complex climate changes, unpredictable weather variations, and continual alterations in surface coverage, the subsystems comprising the atmospheric, soil, and vegetation components in ecohydrological systems undergo corresponding changes in resilience, fragility, and sensitivity. Water moves from the soil through plant roots and stems, eventually reaching the leaves. During photosynthesis, water vapor is released into the atmosphere through open stomata. Stable isotopes of hydrogen and oxygen serve as natural tracers, enabling monitoring of the vertical migration and transformation of water in the ecosystem(Goodwell et al., 2018).

The semi-arid natural environment influences the hydrological processes in the soil-plant-atmosphere continuum. However, the contribution of vegetation transpiration (T) to water fluxes in these mountainous regions, which rely on rainfall and snowmelt as water sources, remains unclear. Furthermore, most studies have focused solely on partitioning evapotranspiration within the ecosystem, which obscures the fate of water vapor. In our research, we analyze the water vapor fluxes from soil evaporation and vegetation transpiration into the atmosphere, which is crucial for understanding water loss dynamics and ensuring appropriate allocation of water resources in the upstream and downstream regions of mountainous areas.

Section 2: The authors should add the area of the catchment and of the study site (it is unclear whether it is a subcatchment, a hillslope or a plot), and more specific topographic characteristics (e.g., elevation range, slope, aspect etc.). Lithology, soil type and texture should be described as well.

Respone: We have made revisions to Section 2 based on your feedback, **as follows:**

2. Study area

The Qilian Mountains are located in the central part of the Eurasian continent, on the northeastern edge of the Qinghai-Tibet Plateau. The eastern region is dominated by water erosion, with large variations in mountainous terrain and an average elevation of over 4,000 meters. Permafrost is developed at elevations of 3,500 to 3,700 meters, and areas above 4,500 meters are characterized by modern glacier development. The region has a plateau continental climate, with hot summers and cold winters, strong solar radiation, and large temperature differences between day and night. The average annual temperature is below 4℃, with extreme highs of 37.6℃ and extreme lows of -35.8℃. The annual sunshine hours range from 2,500 to 3,300 hours, with a total solar radiation of 5,916 to 15,000 megajoules per square meter. The average annual precipitation is 400 millimeters, and the annual evaporation ranges from 1,137 to 2,581 millimeters. The average wind speed is around 2 meters per second, and the frost-free period lasts from 23.6 to 193 days. The Shiyang River originates from the Daxueshan on the northern side of the Lenglong Ridge in the eastern section of the Qilian Mountains, serving as a major water source for the city of Wuwei. The soil types in the eastern section are diverse, but with low organic matter content. The distribution of vegetation shows distinct zonal characteristics, with mountainous forest-grassland zones (2,600 to 3,400 meters), subalpine shrub-meadow zones (3,200 to 3,500 meters), and high mountain sub-ice-snow sparse vegetation zones (>3,500 meters) at elevations above 2,700 meters. The main types of natural forest vegetation include Qinghai spruce forest, Qilian juniper forest, and Chinese pine forest, with Qinghai spruce being the dominant tree species (Zhu et al., 2022).

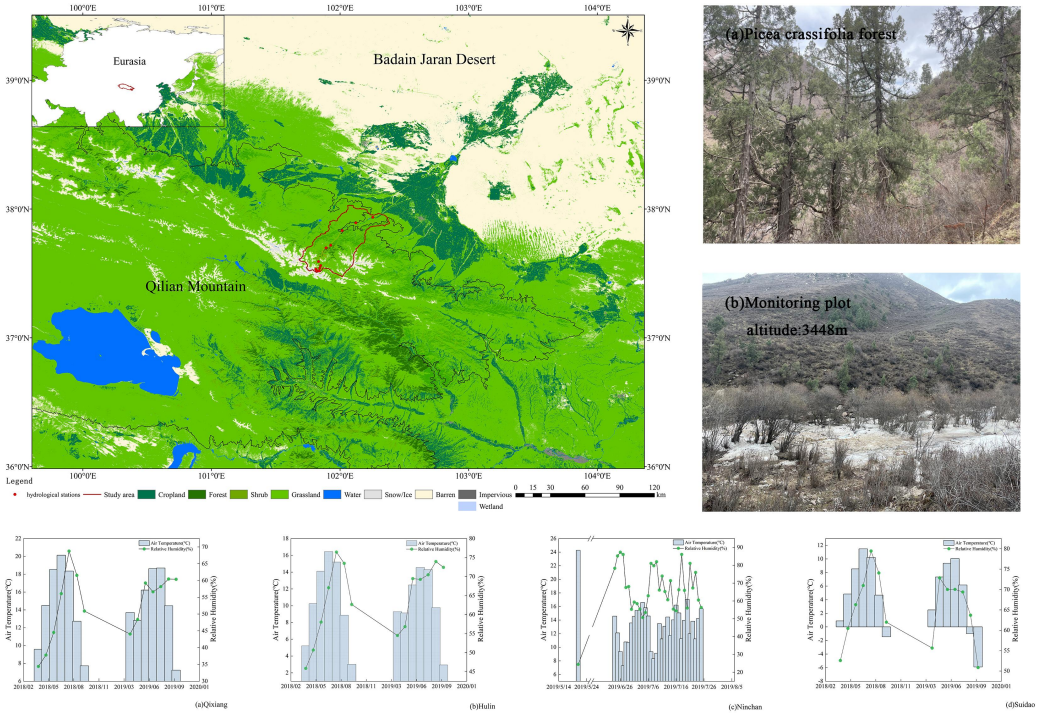

Figure 1 Location of the study area and changes in meteorological conditions

Section 3.1: In this section, the authors should provide clear and detailed information about meteorological data and water sample collection. About meteorological data, the authors should clarify whether the station is located in the study site (is it representative of the local meteorological conditions?) and the temporal resolution of the measurements. About water samples, details should include temporal (monthly, weekly, daily or event timescale?) and spatial resolution (how many locations for each water source? At which elevation?), as well as depth for soil water samples (and how many locations?) and xylem samples (how many trees and locations were considered?). Furthermore, in this section the authors should describe the methodological approaches used for precipitation collection (what kind of collector was used?) and extraction of water samples from soil and plants (what kind of plant tissue was collected?)

Respone: Thank you very much for your meticulous feedback on this section. We have taken your comments seriously and made the following revisions:

1.1 Materials Sources

1.1.1 Sampling network

Table 1 Sampling Point Locations and Sample Quantity Information

Parameter / Station	Qixiang	Hulin	Ninchan	Suidao

	Altitude(m)	2543	2721	3068	3448
Local climate	Temperature(℃/a)	3	3.2	3.3	-0.9
	Precipitation(mm/a)	510	469.44	394	475
	Relative humidity（%/a）	52.9	56.1	66.6	69.2
Samplings number	Precipitation	53	108	91	135
	Soil water	220	560	560	560
	Xylem water	236	56	56	56

3.1.2 Sample collection

We use an automatic weather station in 2018 and 2019 to record meteorological data, in which a rain gauge is used to collect precipitation and transfer samples to 100ml containers after each rain. Drill holes 0 ~ 5 cm, 5 ~ 10 cm, 10 ~ 20 cm, 20 ~ 30 cm, 30 ~ 40 cm, 30 ~ 50 cm, 50 ~ 60 cm, 60 ~ 70 cm, 70 ~ 80 cm, 80 ~ 90 cm, 90 in the sample plot by using soil drill ~ 100 cm. The soil samples were divided into two parts, one of which was placed in a 50 ml glass bottle. The bottle was sealed with a subfilm and transported to the observation station within 10 hours after the sampling date was marked for cryopreservation to detect stable isotope data. The other part of the sample was placed in a 50ml aluminum box and the soil moisture content was determined by drying method. When collecting plant samples, we used scissors to collect vegetation xylem stems, peeled off the bark, and put them in 50ml glass bottles sealed and frozen for experimental analysis.

We utilized the monthly potential evapotranspiration dataset of China, with a spatial resolution of 0.0083333° (approximately 1 km), covering the period from January 1990 to December 2021. The data is measured in units of 0.1 mm. This dataset is derived from the China 1 km monthly mean temperature, minimum temperature, and maximum temperature dataset(Peng et al.,2022;Dinget al.,2020;Ding et al.,2021), using the Hargreaves equation for estimating potential evapotranspiration (Peng et al., 2017). The formula is as follows: P_{ET} = 0.0023 × S0 × (MaxT − MinT)0.5 × (MeanT + 17.8), where P_{ET} represents potential evapotranspiration in mm/month, MaxT, MinT, and MeanT are the monthly maximum temperature,

minimum temperature, and mean temperature, respectively. S0 represents the theoretical solar radiation reaching the top of the Earth's atmosphere, calculated based on solar constant, distance between Earth and the sun, Julian day, and latitude. For data storage convenience, the values are stored as int16 type in NETCDF (nc) files. The surface evapotranspiration data were obtained from the MODIS-based daily surface evapotranspiration data of the Qilian Mountains (2019), with a spatial resolution of 0.01°（Yao et al., 2017;Yao et al., 2020）.

Section 3: This section also lacks a paragraph reporting how water samples were transported and stored before isotopic analyses, and details about laboratory analyses. These details should include the methodology used for isotopic analyses of the different water samples, the uncertainty in the isotopic measurements, any information about protocols used to ensure the quality of the analyses.

Respone: Thank you for your suggestions. We have rewritten this section based on your feedback. Here is the revised version:

3.2 Experimental Analysis

The isotopic data used in this study mainly include stable isotopes of precipitation, soil water, and xylem water. All isotopic samples were analyzed at the Stable Isotope Laboratory of Northwest Normal University. The precipitation samples were analyzed for hydrogen and oxygen stable isotopes using a liquid water isotope analyzer (DLT-100, Los Gatos Research, USA). After thawing the soil and vegetation samples, they were extracted using a low-temperature vacuum condensation device (LI-2100, LICA United Technology Limited, China), and the extracted water was subjected to isotopic analysis. Each water sample was tested six times to ensure accuracy, with the first two tests considered as interference and only the results of the subsequent four tests were averaged (Zhu et al., 2022). The isotopic measurements are represented by δ, which represents the deviation in parts per thousand of the ratio of two stable isotopes in the sample relative to the ratio in a standard sample. The International Atomic Energy Agency (IAEA) defined the Vienna Standard Mean

Ocean Water (VSMOW) in 1968 as the standard for isotopic composition, which is derived from distilled seawater and has a similar isotopic composition to Standard Mean Ocean Water (SMOW).

$$\delta = (\frac{\delta_{Sampling}}{\delta_{Standard}} - 1) \times 1000‰ \quad (1)$$

In Section 3.3.5 and 3.3.6, the authors should clarify if they have assessed the uncertainty in their estimations, for instance, by error propagation and based on the uncertainty in the isotopic analyses and isotopic variability among various samples.

Respone: This is a great question, and we have made modifications to the content based on your feedback. We have addressed the uncertainties related to sections 3.3.5 and 3.3.6 separately in section 5.2 Uncertainty Analysis. Additionally, we have presented how we avoided isotopic variations among samples in section 3.2 Experimental Analysis.

Table 1: The number of xylem water samples (only 7) used for this study is too low. I think these few samples alone cannot support findings and the conclusions

Respone: Your concern is entirely justified, and in the revised manuscript, we have addressed it by adding more sampling points and extending the sampling duration, thus avoiding any potential unreliability in the analysis results. **The additional information on the sampling points is provided below:**

Table 1 Sampling Point Locations and Sample Quantity Information

Parameter	Station	Qixiang	Hulin	Ninchan	Suidao
Local climate	Altitude(m)	2543	2721	3068	3448
	Temperature(℃/a)	3	3.2	3.3	-0.9
	Precipitation(mm/a)	510	469.44	394	475
	Relative humidity（%/a）	52.9	56.1	66.6	69.2

Samplings number	Precipitation	53	108	91	135
	Soil water	220	560	560	560
	Xylem water	236	56	56	56

We have revised the original Table 1 in Section 4.1 and renamed it as Table 2. Furthermore, we have made adjustments to the content of the table.**As follows:**

During the growth season of Qinghai spruce, the stable isotopes of precipitation exhibit specific patterns of fluctuation (Table 2). In the early stages of growth, the hydrogen and oxygen isotope values are generally low. As the temperature gradually increases, the extent of water evaporation and loss intensifies, leading to an enrichment of stable isotopes. The average δ^2H value of precipitation throughout the growth season is -45.52‰, fluctuating roughly between -238.62‰ and 63.43‰. The average δ18O value is -7.75‰, fluctuating roughly between -31.49‰ and 14.79‰. There is not a significant depletion or enrichment of stable isotopes in the wood tissues, with a fluctuation range of -76.95‰ to 23.87‰ for δ^2H and -11.92‰ to 24.77‰ for $\delta^{18}O$. Shallow soil water shows a less pronounced enrichment of heavy isotopes compared to precipitation and wood tissues, with a lower degree of fluctuation observed during late spring and the beginning of summer.

Table 2 Stable isotopes of different water bodies during the growing season

Average / Period	δ^2H/‰			$\delta^{18}O$/‰		
	Precipitation	Xylem water	Soil water（0~10cm）	Precipitation	Xylem water	Soil water（0~10cm）
4	-69.15	-39.02	-53.10	-10.25	2.56	-7.10
5	-39.09	-29.78	-45.38	-7.61	4.44	-6.42
6	-31.29	-45.83	-46.08	-5.74	-2.83	-6.12
7	-32.39	-47.63	-47.71	-5.33	-0.97	-7.06
8	-48.88	-44.55	-68.85	-7.79	-2.06	-9.07
9	-29.38	-42.62	-49.20	-6.46	-1.83	-6.79

10	-68.43	-44.57	-54.88	-11.06	-2.25	-7.96

Figure 3a: The authors report soil depths here, but they should have described those sampling depths in a previous section. Furthermore, the authors should clearly explain why soil depth varies for various sampling times.

Respone: Thank you for your feedback. What I intended to convey here is to utilize soil moisture content at different depths to reflect the information of unbalanced fractionation in soil evaporation. However, it seems that our original figures and sampling points deviated from this intention. **Therefore, we have reorganized this section accordingly, as follows:**

Unsaturated water vapor leads to non-equilibrium fractionation during the process of precipitation, with an average d-excess value of 16.58‰ throughout the growing season (Figure 3, a). In May and September, due to higher relative humidity compared to other periods, the evaporation rate of water vapor is faster. The deuterium values show slow fluctuations from June to August, with significant fluctuations starting from mid-August, indicating that local evaporation is gradually enhanced over time due to the influence of temperature and relative humidity, leading to increased non-equilibrium evaporation. The average lc-excess value of precipitation in the lower layer of forest distribution is -8.18‰, while the average lc-excess value of precipitation in the middle, upper-middle, and canopy layers is close to 0. This is because the fractionation effect of evaporation is more pronounced at lower elevations. At higher elevations, influenced by rainfall and snowmelt, the soil moisture content in all soil layers is above 30% (Figure 3, b). Towards the end of the growing season, as temperatures decrease, tree leaves fall to the forest floor, forming a litter layer that retains moisture in the soil.

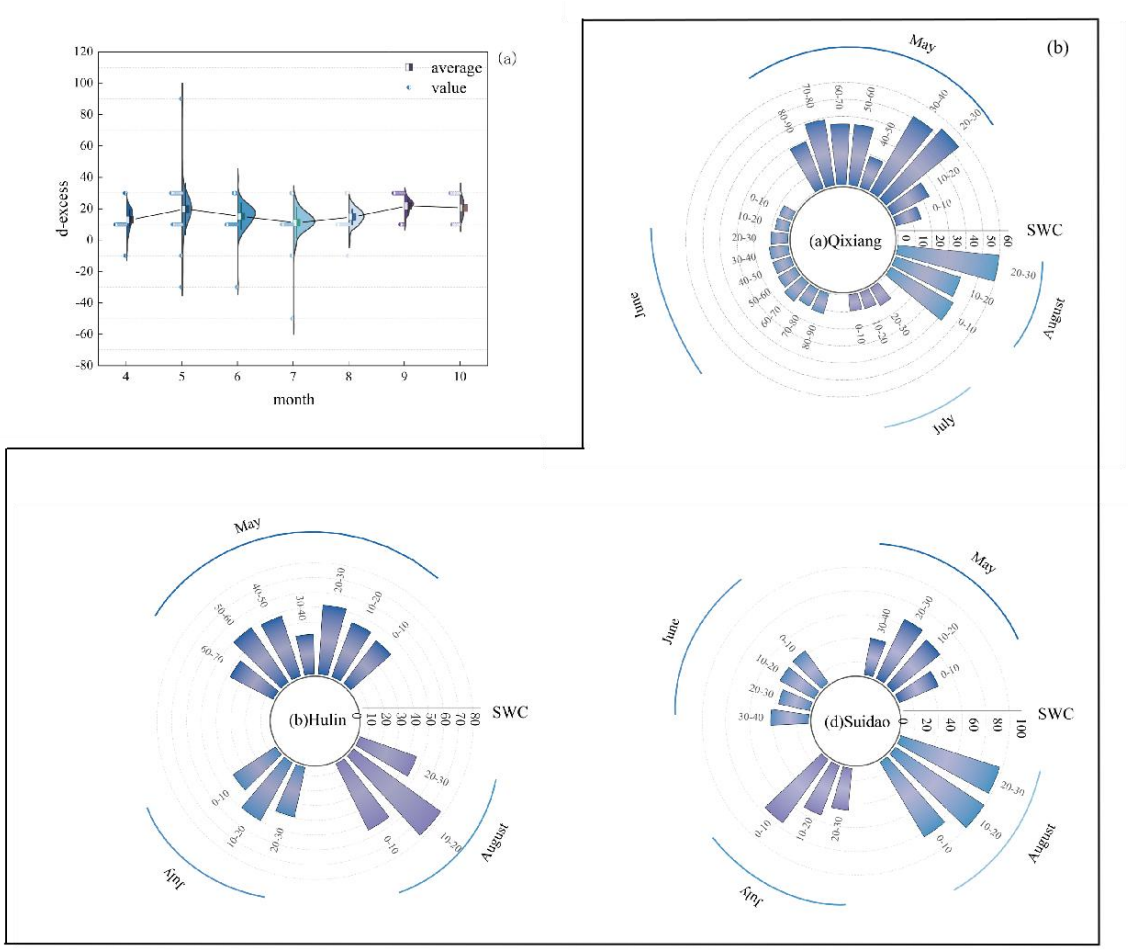

Figure 3 (a) Variation in soil water content, (b) Comparison between atmospheric water vapour oxygen isotopes and d-excess

Figure 7: The authors should indicate the uncertainty in their estimates, clearly in the text and by error bars in this figure.

Respone: Thank you for your feedback. We have restructured section 5.1.2 "Contribution to recirculating water vapor in precipitation" and conducted an analysis of the associated uncertainties. We have also redesigned the tables and figures accordingly. In Figure 7, we have compared the contribution rates of each component only for the growing season. As there are only values available for 7 months for each component, I have not included error bars for visual clarity. I hope you understand

this approach. **As follows:**

5.1.2 Contribution to recirculating water vapour in precipitation

Our previous study in the eastern section of the Qilian Mountains (Zhang et al., 2021) indicated that above an altitude of 2100m, air masses gather from the northern foothills and move along the valley from low to high elevations. From June to August, the atmospheric circulation is influenced by westerlies, southeast monsoons, and plateau monsoons, while from September to October, the westerlies are the dominant factor. Therefore, we selected the Xiying station at an altitude of 2097m as our upwind site. The δ_{pv} values showed depletion in April and October, gradually enriching from June to August. The maximum δ^2H value was -76.02‰ (Table 5), and the minimum was -184.93‰, while the maximum $\delta^{18}O$ value was -11.89‰, and the minimum was -26.38‰. Above 2700 meters, there is a gradual decrease in precipitation vapor with increasing altitude. The δ_{ev} values exhibited significant fluctuations throughout each month, with different patterns at different locations. At 2721m, the δ_{ev} range varied between -172.3‰ and 96.39‰. From the forest's lower layer to the upper layer, the isotopic composition of the advected moisture from the valley gradually diminished, resulting in decreasing values of δ_{adv}.

Table 5 Isotopic Composition of Precipitation Vapor, Surface Evaporation Vapor, and Vegetation Transpiration Vapor at Different Months and Altitudes

Month	Type	isotope	April	May	June	July	August	September	October
Qixiang	δpv	δ^2H/‰	-141.95	-123.83	-99.87	-115.99	-128.34	-120.9	-152.43
		$\delta^{18}O$/‰	-19.27	-16.58	-14.04	-15.91	-18.6	-17.22	-22.34
	δev	δ^2H/‰	-	-125.69	-123.69	-117.98	-134.57	-	-
		$\delta^{18}O$/‰	-	-30.21	-29.56	-28.62	-31.19	-	-
	δtr	δ^2H/‰	-39.9	-29.32	-46.19	-49.58	-45.15	-42.66	-44.64
		$\delta^{18}O$/‰	2.22	-5.87	-4.59	-0.72	-1.72	-1.78	-2.26
	δadv	δ^2H/‰	-145.57	-83.25	-81.12	-92	-109.62	-100.53	-122.62
		$\delta^{18}O$/‰	-20.24	-11.93	-10.73	-12.06	-15.31	-13.46	-18.16
Hulin	δpv	δ^2H/‰	-129.93	-123.29	-98.68	-113.98	-124.16	-118.52	-164.82
		$\delta^{18}O$/‰	-17.54	-16.62	-13.18	-15.48	-17.33	-17.88	-22.46
	δev	δ^2H/‰	-114.24	-117.01	-107.75	-123.44	-106.92	-96.39	-172.3

Ninchan	δtr	$\delta^{18}O$/‰	-14.77	-16.35	-15.03	-16.7	-14.53	-12.78	-24.82
		$\delta^{2}H$/‰	-24.12	-39.62	-35.97	-26.44	-35.85	-38.39	-40.53
	δadv	$\delta^{18}O$/‰	-5.34	-3.58	-4.13	-0.34	-2.35	-4.25	-1.97
		$\delta^{2}H$/‰	-112.79	-115.67	-106.61	-122.19	-106.49	-95.7	-170.54
		$\delta^{18}O$/‰	-14.59	-16.15	-14.88	-16.54	-14.46	-12.69	-24.57
	δpv	$\delta^{2}H$/‰	-	-76.02	-139.21	-135.74	-129.96	-113.71	-184.93
		$\delta^{18}O$/‰	-	-11.89	-19.87	-18.7	-17.91	-16.77	-26.38
	δev	$\delta^{2}H$/‰	-	-83.76	-81.42	-92.42	-110.24	-101.11	-123.42
		$\delta^{18}O$/‰	-	-12.01	-10.76	-12.09	-15.37	-13.49	-18.27
	δtr	$\delta^{2}H$/‰	-	-25.58	-46.77	-37.77	-43.66	-	-
		$\delta^{18}O$/‰	-	-3.45	-1.98	-1.05	-6.68	-	-
	δadv	$\delta^{2}H$/‰	-162.36	-113.49	-111.45	-106.16	-122.12	-114.67	-141.33
		$\delta^{18}O$/‰	-22.73	-15.94	-15.28	-14.46	-16.96	-16.58	-20.42
Suidao	δpv	$\delta^{2}H$/‰	-167.86	-128.08	-124.95	-117.32	-137.73	-130.44	-155.52
		$\delta^{18}O$/‰	-22.9	-18.02	-17.28	-16.04	-19.09	-18.64	-21.59
	δev	$\delta^{2}H$/‰	-164.16	-114.52	-112.37	-106.9	-122.96	-115.47	-142.85
		$\delta^{18}O$/‰	-22.98	-16.07	-15.41	-14.56	-17.08	-16.69	-20.64
	δtr	$\delta^{2}H$/‰	-	-25.58	-46.77	-37.77	-43.66	-	-
		$\delta^{18}O$/‰	-	-8.45	-6.98	-6.05	-6.68	-	-
	δadv	$\delta^{2}H$/‰	-162.38	-113.51	-111.47	-106.18	-122.14	-114.69	-141.36
		$\delta^{18}O$/‰	-22.73	-15.94	-15.28	-14.47	-16.97	-16.58	-20.42

In July, the ratio of vegetation transpiration to precipitation vapor is significantly higher compared to other months. The temperatures in the lower layers of the forest are relatively high, and the middle to upper layers are densely populated with spruce, resulting in a higher f_{tr} (transpiration ratio) throughout the entire growing season. Both the early and late stages of the growing season exhibit noticeably higher f_{ev} (evaporation ratio) compared to other months, with the middle and upper parts of the forest having a higher proportion of evaporated vapor. The average f_{adv} (advected vapor ratio) is 72%, with contributions exceeding 70% for all months except June and July (Figure 7).

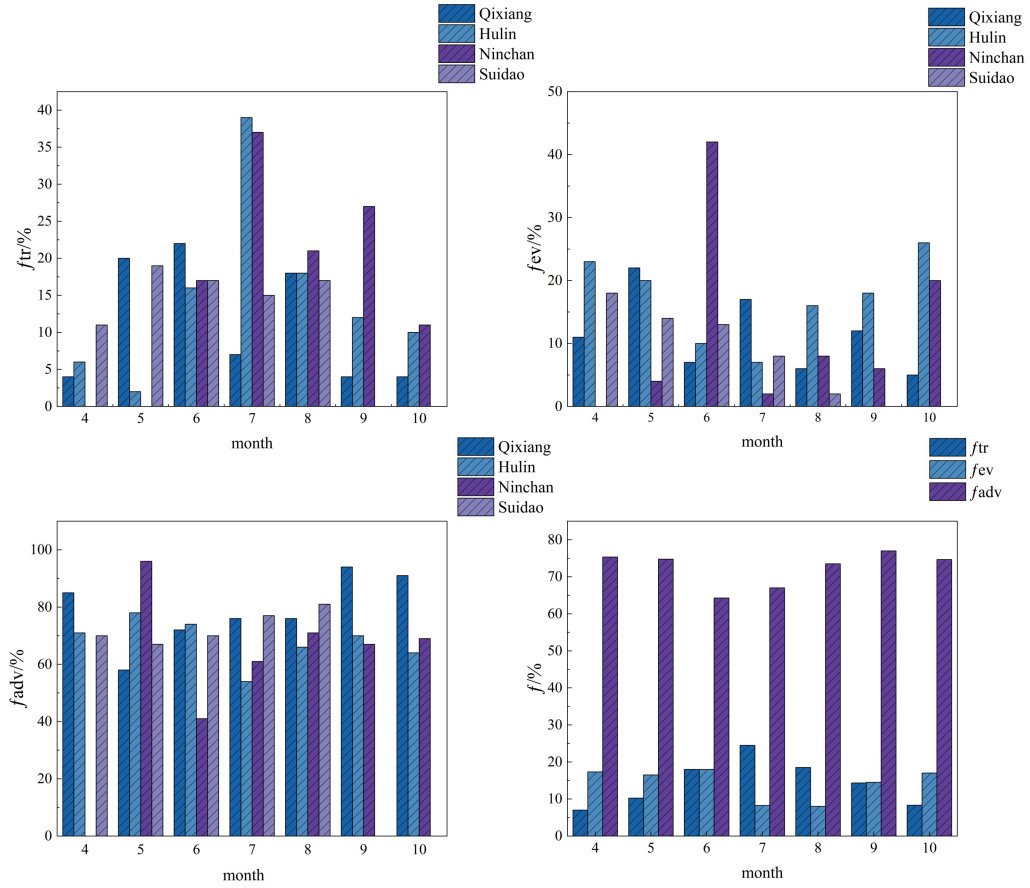

Figure 7 Comparison of f_{adv} (advective water vapour contribution), f_{ev} (surface evaporation water vapour contribution) and f_{tr} (plant transpiration water vapour contribution) for each of period

I do not understand the purpose of Section 5.2 and the title does not reflect the content of the section.

Respone:I completely agree with your viewpoint, and therefore, I have removed that section from the manuscript. Instead, I have revised section 5.2 to focus on uncertainty analysis. **As follows:**

5.2 Uncertainty analysis

A higher sample size can reduce the margin of error. Therefore, we utilized isotopic data from four sites over a two-year period to evaluate the model. We used 404 xylem samples to calculate the contribution ratio of transpiration to ecosystem evapotranspiration. We examined the uncertainty of the model evaluation. When analyzing the evaporation characteristics in a semi-arid natural environment using the Craig-Gordon isotopic model, we first eliminated the influence of solar radiation and other meteorological variables on the calculation results. We focused on temperature, relative humidity, water vapor, and the initial isotopic values of water bodies. Particularly in semi-arid environments, the variations in temperature and relative humidity are crucial (Hernández-Pérez et al., 2020). To verify the calculation results, we found a strong correlation between the isotopes of soil evaporation and relative humidity, as demonstrated by the fitting of δ_E against relative humidity and temperature. This also indicates the reliability of the results obtained through the Craig-Gordon isotopic model. We employed the Keeling plot method to calculate δ_{ET}, which is based on isotopic mass balance and a two-endmember mixing model. This method assumes that the isotopic composition of the background atmosphere and source remains constant, with a very low probability of isotopic spatial variation (Good et al., 2012; Kool et al., 2014). Due to the higher reliability of oxygen isotopes compared to hydrogen isotopes (Han et al., 2022; Kale et al., 2022), we solely used oxygen isotopes to calculate the T/ET values. The results indicate that transpiration significantly outweighs evaporation during July and August, which aligns with previous research findings (Zhu et al., 2022). The correlation between T/ET and soil moisture content suggests that soil moisture is a crucial factor driving the variations in transpiration and evaporation ratios. Additionally, the estimation of isotopic composition of advected water vapor from the upwind sites contributes to increased uncertainty. In our study area, the sites are predominantly influenced by valley winds, with water vapor moving from the valley bottom to higher altitudes.

Therefore, we selected lower elevation areas in the valley bottom as the source region for advected water vapor (Zhang et al., 2021).

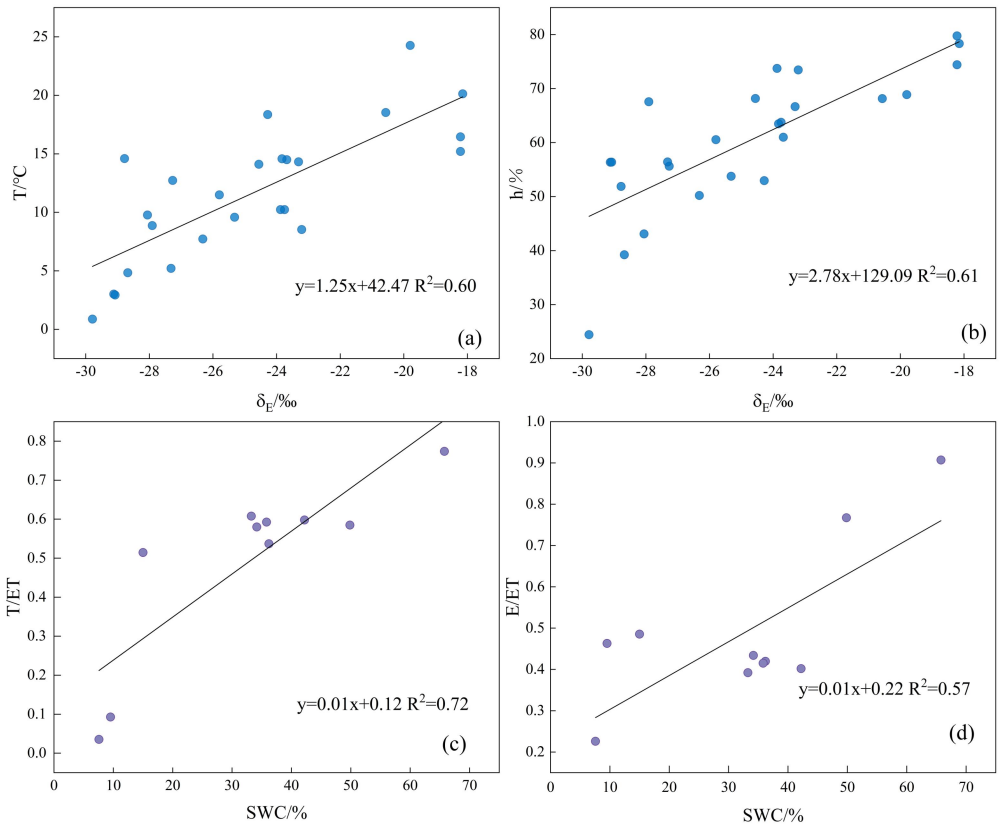

Figure 8 Correlation analysis of factors affecting uncertainty in impact assessment

Technical corrections

- Figure 1: Labels are difficult to read. I suggest increasing their size and resolution.

- Line 107: “Water isotopes…were observed” is an unusual phrasing; please change the verb.

- Figure 2: Again, labels are difficult to read. I suggest increasing their size and resolution.

- Figure 3, 4, 5 and 7: Please increase the size of the labels.

- Figure 8a: The legend is unreadable; please increase the size and the resolution of the labels.

Respone: We have carefully addressed your feedback regarding the figures. In order to enhance the overall quality of the paper, we have recreated all the figures in our manuscript, removing any inappropriate sentences.

We would like to invite you to review the significant changes we have made in the revised manuscript. Attached below is the PDF of the manuscript:

Hydrological effects of evapotranspiration in the Qilian Mountains forest belt

Yinying Jiao[1,2], Guofeng Zhu[1,2*], Dongdong Qiu[1,2], Yuwei Liu[1,2], Lei Wang[1,2], Siyu Lu[1,2], Gaojia Meng[1,2], Xinrui Lin[1,2], Rui Li[1,2],Qinqin Wang[1,2], Longhu Chen[1,2], Niu Sun[1,2]

[1] School of Geography and Environment Science, Northwest Normal University, Lanzhou 730070, Gansu, China

[2] Shiyang River Ecological Environment Observation Station, Northwest Normal University, Lanzhou 730070, Gansu, China

Abstract: Mountainous regions play a crucial role as primary water sources and origins of rivers. The changing climate patterns worldwide are altering the distribution of vegetation and water utilization methods. Hence, gaining a comprehensive understanding of evapotranspiration in mountainous forest zones is essential for comprehending the ecohydrological impact of vegetation and its influence on the water cycle within the watershed. We collected precipitation, soil water from 0 to 100cm, xylem water from Qinghai Spruce, temperature, relative humidity and rainfall in the eastern Qilian Mountains from 2018 to 2019. We simulated T/ET comprehensively, and quantified the contribution of recirculated water vapor in precipitation. The aim of this study was to clarify the evapotranspiration process and its effect on production and confluence in the forest belt of Qilian Mountain. The study revealed that transpiration from Qinghai spruce trees constituted the largest portion of evapotranspiration within the entire Qinghai spruce forest ecosystem, averaging 57%. This indicates that transpiration surpasses evaporation during the growing season. Soil water content and air humidity emerged as the primary factors influencing evapotranspiration within the Qinghai spruce forest zones. Throughout each month of the growing season, evapotranspiration from Qinghai spruce was found to exceed precipitation.Water loss through evapotranspiration is much greater than

water inputs from precipitation and surface water replenishment. Consequently, the forest zone does not yield flows in the eastern part of the Qilian Mountains. The warming of global temperatures and human activities are likely to trigger shifts in the distribution areas and evapotranspiration regimes of Qinghai spruce, which in turn will lead to a change in water resource patterns in the basin.

Keywords: Qinghai spruce; stable isotopes; end-member mixing model; evapotranspiration partitioning

1. Introduction

Future droughts are likely to be more frequent, more severe, and longer-lasting than in recent decades.Under the influence of climate change, in ecologically fragile areas, particularly in arid and semi-arid regions, these changes will be the most rapid and extreme (Ault et al., 2020). As a natural reservoir and purifier, the Qinghai spruce ecosystem has the functions of storing, releasing and purifying water. The Qilian Mountains supply the water resources that human beings depend on for survival in the continental river basin in the arid region, regulate the water cycle in the arid region, and interact with the soil and atmosphere to form a vertical spatial continuum, which not only affects the ecological process of the local plant community, but also changes the regional microclimate by means of latent heat (Zhang et al.,2021). As a water source for several inland rivers, the Qilian Mountains are an important ecological security barrier and a priority area for biodiversity conservation in central Asia. The spruce forest ecosystem provides various ecological, climatic, and social benefits to the Qilian Mountains but is highly vulnerable to drought and temperature extremes. More to the point, climate drivers put spruce forests at risk from drought and heat stress. As the magnitude of climate change increases, the disturbance to its ecosystem is also expected to be higher. The interaction between soil and vegetation controls rainfall input and water transfer within ecosystem components. It is an important player in climate change mitigation in terms of climate benefits (Rohatyn et al., 2022). In the face of complex climate changes, unpredictable weather variations, and continual alterations in surface coverage, the subsystems comprising the atmospheric,

soil, and vegetation components in ecohydrological systems undergo corresponding changes in resilience, fragility, and sensitivity. Water moves from the soil through plant roots and stems, eventually reaching the leaves. During photosynthesis, water vapor is released into the atmosphere through open stomata. Stable isotopes of hydrogen and oxygen serve as natural tracers, enabling monitoring of the vertical migration and transformation of water in the ecosystem(Goodwell et al., 2018).

Evapotranspiration (ET) is an indispensable part of the terrestrial water and energy cycle. Therefore, exploring the spatio-temporal and component changes of soil evaporation and vegetation transpiration can help us increase the response of vegetation canopy to climatechange (Liu et al., 2022). At the ecosystem scale, many studies have classified evapotranspiration (ET) as transpiration (T) and evapotranspiration (E) (Schlesinger et al.,2014). The measurement of evapotranspiration (ET) in field research is often based on physical evaporation from the soil surface and biological transpiration, which involves the uptake of soil water by roots and the loss of water vapor through plant stomata during photosynthesis. Some studies have classified evaporation (E) and transpiration (T) by analyzing the isotopic composition of oxygen in soil and runoff, finding that $\delta^{18}O$ enrichment is primarily associated with evaporation rather than transpiration (Wershaw et al., 1966). Differentiating between soil evaporation and stomatal plant evapotranspiration is a challenging yet crucial task for assessing biomass production and allocating scarce water resources effectively. Generally, plant evapotranspiration (T) is the desired component of water that enhances plant productivity, while soil evaporation (E) is considered a source of water loss or inefficiency. The magnitude of soil evaporation can be significant in sparsely vegetated systems, especially in arid regions or very wet systems such as surface irrigated crops and wetlands (Liu et al., 2015; Zhang et al., 2018). Zoning evapotranspiration is essential for accurately monitoring system hydrology and implementing improved water management practices in these specific scenarios (Kool et al., 2014). Quantifying the role of regional evapotranspiration in the terrestrial water balance and the global water cycle is therefore critical.

On regional and global scales, there are various methods employed to partition

evapotranspiration. Firstly, in river basins, researchers investigate the role of lateral groundwater flow in distributing evapotranspiration by utilizing comprehensive continental-scale hydrological models. These models couple vegetation and land energy processes with surface and underground hydrology to study the distribution of evapotranspiration at the continental scale (Maxwell et al., 2016). Secondly, remote sensing-based approaches are employed to identify differences in evapotranspiration partitioning among different models (Talsma et al., 2018; Chen et al., 2022). Thirdly, eddy covariance methods are utilized to assess multi-year energy fluxes and evapotranspiration in typical alpine meadows, exploring the environmental and biophysical controls on evapotranspiration (Chang et al., 2022). Additionally, studies synthesize available literature data to establish quantitative relationships between evapotranspiration allocation and vegetation cover indices (such as leaf area index, or LAI) in agricultural and natural systems. These studies aim to explain observed changes in T/ET at global scales (Wang et al., 2014; Wei et al., 2018; Cui et al., 2021). The semi-arid natural environment influences the hydrological processes in the soil-plant-atmosphere continuum. However, the contribution of vegetation transpiration (T) to water fluxes in these mountainous regions, which rely on rainfall and snowmelt as water sources, remains unclear. Furthermore, most studies have focused solely on partitioning evapotranspiration within the ecosystem, which obscures the fate of water vapor. In our research, we analyze the water vapor fluxes from soil evaporation and vegetation transpiration into the atmosphere, which is crucial for understanding water loss dynamics and ensuring appropriate allocation of water resources in the upstream and downstream regions of mountainous areas.

As a vascular plant species, Qinghai spruce forests are one of the important entry points for energy and materials in the environment into terrestrial ecosystems. Their growth, survival, and reproduction affect other species' ecological functions and forms within and outside their habitats. There is a high degree of responsiveness between the vegetation, drought resilience, and microclimatic conditions of forests and their ecosystems (Eisenhauer et al., 2021). In this study, we observed and analyzed the monthly xylem water, soil water, precipitation stable isotopes and soil

water content of Spruce forest in the eastern Qilian Mountains from April to October 2018 and 2019, and used these data to solve the following problems: (1) Quantify the contribution rates of soil evaporation and vegetation transpiration to evapotranspiration of ecosystems; (2) Quantifying the ratio of recirculated water vapor in precipitation; (3) To investigate the evapotranspiration process and its influence on production and confluence in the forest belt of Qilian Mountain. This study provides an effective basis for local water resource use and ecological protection.

2. Study area

The Qilian Mountains are located in the central part of the Eurasian continent, on the northeastern edge of the Qinghai-Tibet Plateau. The eastern region is dominated by water erosion, with large variations in mountainous terrain and an average elevation of over 4,000 meters. Permafrost is developed at elevations of 3,500 to 3,700 meters, and areas above 4,500 meters are characterized by modern glacier development. The region has a plateau continental climate, with hot summers and cold winters, strong solar radiation, and large temperature differences between day and night. The average annual temperature is below 4℃, with extreme highs of 37.6℃ and extreme lows of -35.8℃. The annual sunshine hours range from 2,500 to 3,300 hours, with a total solar radiation of 5,916 to 15,000 megajoules per square meter. The average annual precipitation is 400 millimeters, and the annual evaporation ranges from 1,137 to 2,581 millimeters. The average wind speed is around 2 meters per second, and the frost-free period lasts from 23.6 to 193 days. The Shiyang River originates from the Daxueshan on the northern side of the Lenglong Ridge in the eastern section of the Qilian Mountains, serving as a major water source for the city of Wuwei. The soil types in the eastern section are diverse, but with low organic matter content. The distribution of vegetation shows distinct zonal characteristics, with mountainous forest-grassland zones (2,600 to 3,400 meters), subalpine shrub-meadow zones (3,200 to 3,500 meters), and high mountain sub-ice-snow sparse vegetation zones (>3,500 meters) at elevations above 2,700

meters. The main types of natural forest vegetation include Qinghai spruce forest, Qilian juniper forest, and Chinese pine forest, with Qinghai spruce being the dominant tree species (Zhu et al., 2022).

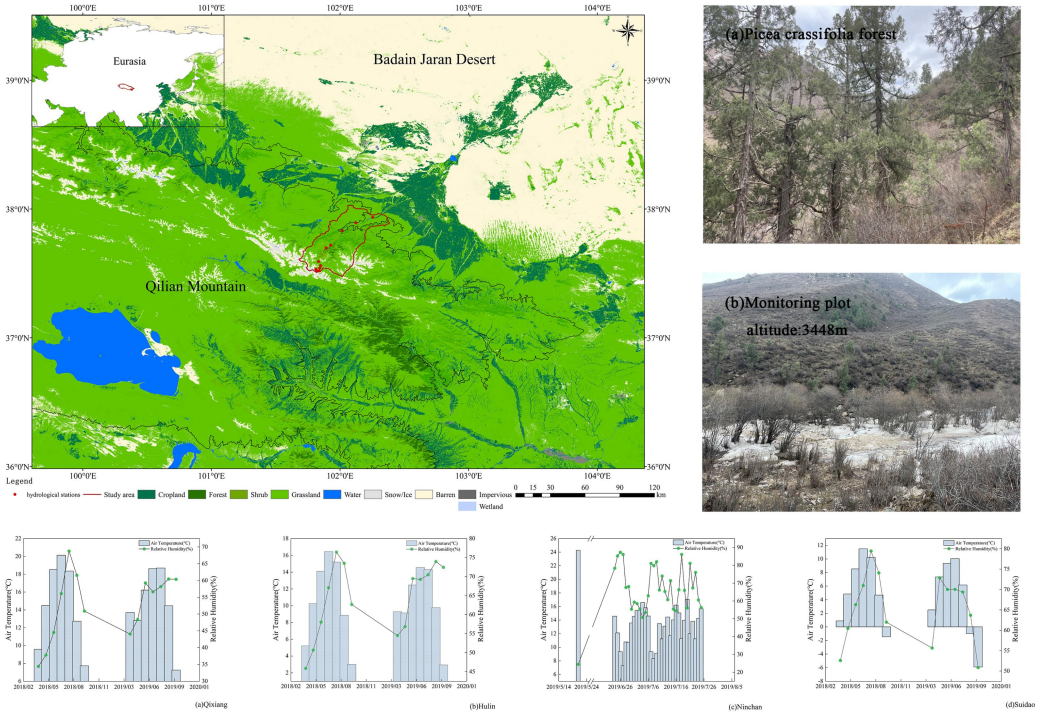

Figure 1 Location of the study area and changes in meteorological conditions

3. Materials and methods

3.1 Materials Sources

3.1.1 Sampling network

Table 1 Sampling Point Locations and Sample Quantity Information

Parameter	Station	Qixiang	Hulin	Ninchan	Suidao
	Altitude(m)	2543	2721	3068	3448
Local climate	Temperature(℃/a)	3	3.2	3.3	-0.9
	Precipitation(mm/a)	510	469.44	394	475
	Relative humidity（%/a）	52.9	56.1	66.6	69.2
Samplings number	Precipitation	53	108	91	135
	Soil water	220	560	560	560
	Xylem water	236	56	56	56

3.1.2 Sample collection

We use an automatic weather station in 2018 and 2019 to record meteorological data, in which a rain gauge is used to collect precipitation and transfer samples to 100ml containers after each rain. Drill holes 0 ~ 5 cm, 5 ~ 10 cm, 10 ~ 20 cm, 20 ~ 30 cm, 30 ~ 40 cm, 30 ~ 50 cm, 50 ~ 60 cm, 60 ~ 70 cm, 70 ~ 80 cm, 80 ~ 90 cm, 90 in the sample plot by using soil drill ~ 100 cm. The soil samples were divided into two parts, one of which was placed in a 50 ml glass bottle. The bottle was sealed with a subfilm and transported to the observation station within 10 hours after the sampling date was marked for cryopreservation to detect stable isotope data. The other part of the sample was placed in a 50ml aluminum box and the soil moisture content was determined by drying method. When collecting plant samples, we used scissors to collect vegetation xylem stems, peeled off the bark, and put them in 50ml glass bottles sealed and frozen for experimental analysis.

We utilized the monthly potential evapotranspiration dataset of China, with a spatial resolution of 0.0083333° (approximately 1 km), covering the period from January 1990 to December 2021. The data is measured in units of 0.1 mm. This dataset is derived from the China 1 km monthly mean temperature, minimum temperature, and maximum temperature dataset(Peng et al.,2022;Dinget al.,2020;Ding et al.,2021), using the Hargreaves equation for estimating potential evapotranspiration (Peng et al., 2017). The formula is as follows: $P_{ET} = 0.0023 \times S0 \times (MaxT - MinT)0.5 \times (MeanT + 17.8)$, where P_{ET} represents potential evapotranspiration in mm/month, MaxT, MinT, and MeanT are the monthly maximum temperature, minimum temperature, and mean temperature, respectively. S0 represents the theoretical solar radiation reaching the top of the Earth's atmosphere, calculated based on solar constant, distance between Earth and the sun, Julian day, and latitude. For data storage convenience, the values are stored as int16 type in NETCDF (nc) files. The surface evapotranspiration data were obtained from the MODIS-based daily surface evapotranspiration data of the Qilian Mountains (2019), with a spatial resolution of 0.01°（Yao et al., 2017;Yao et al., 2020）.

3.2 Experimental Analysis

The isotopic data used in this study mainly include stable isotopes of precipitation, soil water, and xylem water. All isotopic samples were analyzed at the Stable Isotope Laboratory of Northwest Normal University. The precipitation samples were analyzed for hydrogen and oxygen stable isotopes using a liquid water isotope analyzer (DLT-100, Los Gatos Research, USA). After thawing the soil and vegetation samples, they were extracted using a low-temperature vacuum condensation device (LI-2100, LICA United Technology Limited, China), and the extracted water was subjected to isotopic analysis. Each water sample was tested six times to ensure accuracy, with the first two tests considered as interference and only the results of the subsequent four tests were averaged (Zhu et al., 2022). The isotopic measurements are represented by δ, which represents the deviation in parts per thousand of the ratio of two stable isotopes in the sample relative to the ratio in a standard sample. The International Atomic Energy Agency (IAEA) defined the Vienna Standard Mean Ocean Water (VSMOW) in 1968 as the standard for isotopic composition, which is derived from distilled seawater and has a similar isotopic composition to Standard Mean Ocean Water (SMOW).

$$\delta = \left(\frac{\delta_{Sampling}}{\delta_{Standard}} - 1\right) \times 1000‰ \quad (1)$$

3.3 Research methods

3.3.1 Isotopic composition of atmospheric water vapour

The stable isotope composition of moisture in ambient air is calculated as follows(Gibson and Reid, 2014;Skrzypek et al., 2015):

$$\delta_A = \frac{\delta_{rain} - k\varepsilon^+}{1 + k\alpha^+ \times 10^{-3}} \quad (2)$$

where k=1, or by fitting k to some fraction of 1 as the best fit to the local evaporation line, is the isotopic fractionation factor. Defined by $\varepsilon^+ = (\alpha^+ - 1) \times 1000$. α^+about ^2H and ^{18}O are calculated as follows(Horita and Wesolowski, 1994):

$$10^3\ln^2\alpha^+ = 1158.8T^3/10^9 - 1620.1T^2/10^6 + 794.84T/10^3 - 161.04 + 2.9992 \times 10^9/T^3 \quad (3)$$

$$10^3\ln^{18}\alpha^+ = -7.685 + 6.7123\times 10^3/T - 1.6664\times 10^6/T^2 + 0.35041 \times 10^9/T^3 \quad (4)$$

3.3.2 Isotopic composition of soil evaporation

The Craig-Gordon model was used to calculate the stable isotopic composition of soil evaporation water vapour, δ_E, using the following equation(Craig and Gordon, 1965;Yepez et al., 2005).

$$\delta_E = \frac{\alpha_e^{-1}\delta_s - h\ \delta_A - \varepsilon_{eq} - (1-h\ )\varepsilon_k}{(1-h\ ) + 10^{-3}(1-h\ )\varepsilon_k} \quad (5)$$

where α_e(>1) is the equilibrium factor calculated as a function of water surface temperature, δs is the stable isotopic composition of liquid water at the evaporating surface of the soil (0 ~ 10 cm average stable isotopic composition of soil water), δ_A is the stable isotopic composition of atmospheric water vapour near the surface, εeq represents the equilibrium fractionation corresponding to $\varepsilon eq = (1\text{-}1/\alpha e) \times 1000$, εk is the kinetic fractionation factor of O^2 is approximately 18.9‰ and h is the atmospheric relative humidity(Gibson and Reid, 2010). For $\delta^{18}O$, α_e is calculated as follows(Raz-Yaseef et al., 2010):

$$\alpha_e = \frac{1.137\times 10^6/T^2 - 0.4156\times 10^3/T - 2.0667}{1000} + 1 \quad (6)$$

Where T is the soil Kelvin temperature (K) at a depth of 5 cm.

3.3.3 Isotopic composition of plant transpiration

When transpiration is strong, leaf water is in "isotopic stable state", that is, the isotopic composition of leaf transpiration water is equivalent to that of water absorbed by the roots of rain plants at noon. Therefore, the stable isotopic composition of water in plant xylem can be used to represent the stable isotopic composition of water vapor in plant transpiration. The expression is as follows(Aron et al., 2020):

$$\delta_T = \delta_X \quad (7)$$

where δ_x is the isotopic ratio of xylem water and δ_T is the isotopic ratio of

transpiration.

3.3.4 Evapotranspiration isotope assessment

The Keeling Plot model describes the linear relationship between the oxygen isotope composition of atmospheric water vapour and its reciprocal concentration . The intercept of the curve on the Y-axis represents the oxygen isotopic composition of evapotranspiration (δ_{ET}) and is expressed as(Keeling, 1958;Wang et al., 2015):

$$\delta_a = \frac{C_b(\delta_b - \delta_{ET})}{C_a} + \delta_{ET} \quad (8)$$

Where δ_a and C_a represent the atmospheric water vapour oxygen isotopic composition (‰) and water vapour concentration in the ecosystem boundary layer, δ_b and C_b represent the background atmospheric water vapour oxygen isotopic composition and background atmospheric water vapour concentration, and δ_{ET} is the ecosystem evapotranspiration oxygen isotopic composition.

3.3.5 Ecosystem evapotranspiration partitioning

The determination of evapotranspiration by means of biotic and abiotic isotopic composition can be used to improve the understanding of community structure and ecosystem function in Qinghai spruce forests in the Qilian Mountains. Based on the isotope mass balance approach to consider the distribution of major and minor isotopes, the partitioning of evapotranspiration can be achieved using two end-member mixing models (E and T) with the following expression(Kool et al.,2014;Wei et al., 2018):

$$\frac{T}{ET} = \frac{\delta_{ET} - \delta_E}{\delta_T - \delta_E} \quad (9)$$

where δ_{ET}, δ_E and δ_T are the isotopic compositions of evapotranspiration (ET), soil evapotranspiration (E) and plant evapotranspiration (T), respectively, and the isotopic values of the three can be obtained by both direct observation and model estimation.

3.3.6 Three-component mixing model

Assuming that precipitation vapor is a mixture of advective water vapour and recirculating water vapour, it is understood that the proportion of both precipitation and precipitation water vapour has the same nature. The proportion of precipitation

occupied by advective vapour is calculated as follow(Kong et al., 2013; Wang et al., 2022):

$$f_{re} = \frac{P_{tr}+P_{ev}}{P_{tr}+P_{ev}+P_{adv}} \quad (10)$$

where P_{tr}, P_{ev} and P_{adv} are precipitation produced by transpiration, surface evaporation and advection, respectively.

This can be calculated using the following formula(Brubaker et al., 1993; Sang et al., 2023):

$$\delta_{pv} = \delta_{tr} f_{tr} + \delta_{ev} f_{ev} + \delta_{adv} f_{adv} \quad (11)$$

$$f_{ev} + f_{tv} + f_{adv} = 1 \quad (12)$$

where f_{tr}, f_{ev} and f_{adv} are the proportional contributions of transpiration, surface evaporation and advection to precipitation, respectively, and δ_{pv}, δ_{tr}, δ_{ev} and δ_{adv} values are the stable isotopes in precipitating transpiration, transpiration, surface evaporation and advective vapour, respectively. f_{tr},f_{ev} and f_{adv} are calculated by Isoerror software, based on dual isotopes and three sources(Ver. 1.3.1, https://www.epa.gov/)(Phillips and Gregg, 2001). δpv is calculated using the following formula:

$$\delta_{pv} = \frac{\delta_p - k\varepsilon^+}{1+k\varepsilon^+} \quad (13)$$

Using the C-G model to calculate δ_{ev}, the formula is as follows:

$$\delta_e = \frac{\delta_s/\alpha^+ - h\delta_{adv} - \varepsilon}{1-h+\varepsilon_k} \quad (14)$$

Including the δs is the isotopic composition of liquid water evaporation front, δ_{adv} is advection steam, h is relative humidity, α^+ is equilibrium fractionation factor, ε_k is kinetic fractionation factor, Ɛ is total fractionation factor.

$$\varepsilon = \varepsilon^+/\alpha^+ + \varepsilon_k \quad (15)$$

$$\varepsilon_k = (1-h)\theta_n C_k \quad (16)$$

h is the relative humidity, C_k is the kinetic fractionation constant, δ^2H is 25.1‰, $\delta^{18}O$ is 28.5‰.The weight coefficient θ of small water body is 1, and θ of large water body is 0.5. n ranges from 0.5 (fully turbulent transport, with reduced kinetic fractionation, suitable for lake or saturated soil conditions) to 1 (fully diffused transport, suitable for very dry soil conditions), with a kinetic fractionation coefficient

of about 12.2-24.5‰ for ε_k (^2H) in a dry atmosphere (h=0). The kinetic separation coefficient of εk (^{18}O) is about 13.8-27.7‰.

The advection water vapor isotope δ_{adv} in the three-component mixing model needs to be determined by the water vapor isotopic composition at the upwind position. Based on the HYSPLIT model, we found that the eastern Qilian Mountains was controlled by westerly winds, southeast monsoon and plateau monsoon in June, July and August, and by prevailing westerly winds in September and October. The clustering analysis of air masses in different months shows that air masses accumulate at the northern foot of Qilian Mountains and move from low altitude to high altitude along the valley. Xiying, at 2097 m above sea level, is therefore used as a headwind station from April to October. When steam isotopes show a depletion trend along the transport path, isotopic fractionation is assumed to be due to Rayleigh distillation, and the expression is as follow:

$$\delta_{adv} = \delta_{pv-adv} + (\alpha^+ - 1)\ln F \quad (17)$$

Where $\delta_{pv\text{-}adv}$ is the isotopic composition in the vapor of the winds tation, and F is the ratio between the final vapor and the initial vapor. Since rainfall is positively correlated with the surface vapor pressure of the whole study area (c=1.657e, where c is the water vapor content in mm, e is the surface vapor pressure in hPa, R^2=0.94), we used the surface vapor pressure of each site to calculate the value of F. The recirculated water entering the air mass is not considered here, because the contribution of recirculated water to the total air column is very limited, and most of the available precipitation does not result in rainfall but escapes to other areas. If there is no depletion of isotope ratios along the transmission track, the vapor isotope ratio from the upwind station is applied directly, and the Rayleigh distillation equation is not applied.

The δp is corrected by the local evaporation line (LEL), and the LEL slope (SLEL) can be calculated as（Skrzypek et al.，2015):

$$S_{LEL} = \frac{(h-10^{-3}{}^{18}\varepsilon)[h(\,{}^{2}\delta_{pv} - {}^{2}\delta_{p}) + {}^{2}\varepsilon(1+10^{-3}\,{}^{2}\delta_{pv})}{(h-10^{-3}\,{}^{2}\varepsilon)[h({}^{18}\delta_{pv} - {}^{18}\delta_{p}) + {}^{18}\varepsilon(1+10^{-3}{}^{18}\delta_{p})]} \quad (18)$$

Where h is the relative humidity, Ɛ is the total fractionation factor, and δ_{PV} and δ_P are the stable isotopic components of water vapor and precipitation.According to our research results, the LEL equation for the study area is $\delta^2H=3.86\delta^{18}O-19.88$ ($R^2=0.994$, $P < 0.0001$, n=19).

4. Results and analysis

4.1 Hydrogen and oxygen isotope variations in different water bodies

During the growth season of Qinghai spruce, the stable isotopes of precipitation exhibit specific patterns of fluctuation (Table 2). In the early stages of growth, the hydrogen and oxygen isotope values are generally low. As the temperature gradually increases, the extent of water evaporation and loss intensifies, leading to an enrichment of stable isotopes. The average δ^2H value of precipitation throughout the growth season is -45.52‰, fluctuating roughly between -238.62‰ and 63.43‰. The average δ18O value is -7.75‰, fluctuating roughly between -31.49‰ and 14.79‰. There is not a significant depletion or enrichment of stable isotopes in the wood tissues, with a fluctuation range of -76.95‰ to 23.87‰ for δ^2H and -11.92‰ to 24.77‰ for $\delta^{18}O$. Shallow soil water shows a less pronounced enrichment of heavy isotopes compared to precipitation and wood tissues, with a lower degree of fluctuation observed during late spring and the beginning of summer.

Table 2 Stable isotopes of different water bodies during the growing season

Average / Period	δ^2H/‰			$\delta^{18}O$/‰		
	Precipitation	Xylem water	Soil water (0~10cm)	Precipitation	Xylem water	Soil water (0~10cm)
4	-69.15	-39.02	-53.10	-10.25	2.56	-7.10
5	-39.09	-29.78	-45.38	-7.61	4.44	-6.42
6	-31.29	-45.83	-46.08	-5.74	-2.83	-6.12
7	-32.39	-47.63	-47.71	-5.33	-0.97	-7.06

8	-48.88	-44.55	-68.85	-7.79	-2.06	-9.07
9	-29.38	-42.62	-49.20	-6.46	-1.83	-6.79
10	-68.43	-44.57	-54.88	-11.06	-2.25	-7.96

LMWL exhibits variations across different vertical gradients, primarily influenced by temperature and humidity. It is noteworthy that relative humidity is generally low at all four heights within the forest, resulting in local meteoric water lines (LMWL) being lower than the global meteoric water line (GMWL). At an elevation of 2543m, which represents the lowest layer of tree growth, the temperature can reach up to 20℃ in July, and the slope of the local meteoric water line (LMWL) is 6.74. At 2721m, the average temperature throughout the growing season is 10.4℃, with a maximum temperature of 16.45℃ in July and an average relative humidity of 64.38%. The slope of LMWL is 7.02 (Figure 2, d). At the Suidao station located at an elevation of 3448m, the slope of the precipitation regression line is 7.75, which is close to the slope of the GMWL but exhibits the largest deviation from the local evaporation line (Figure 2, a). The soil water line (SWL) in the forest's lower layer is smaller and closer to the local evaporation line, indicating stronger evaporative fractionation and dynamic fractionation compared to the other three sampling zones. The slopes of the SWL are smaller than the slopes of LMWL, indicating that precipitation is the main source of soil moisture replenishment.

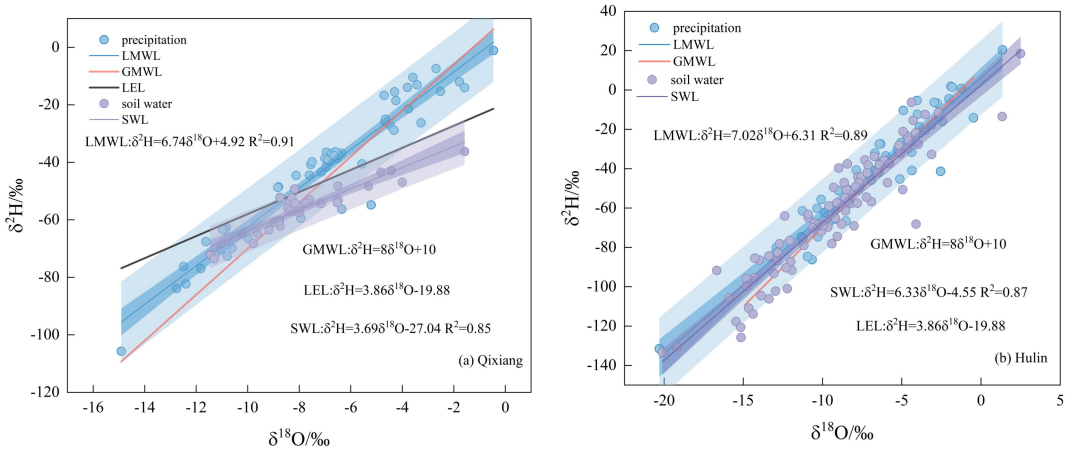

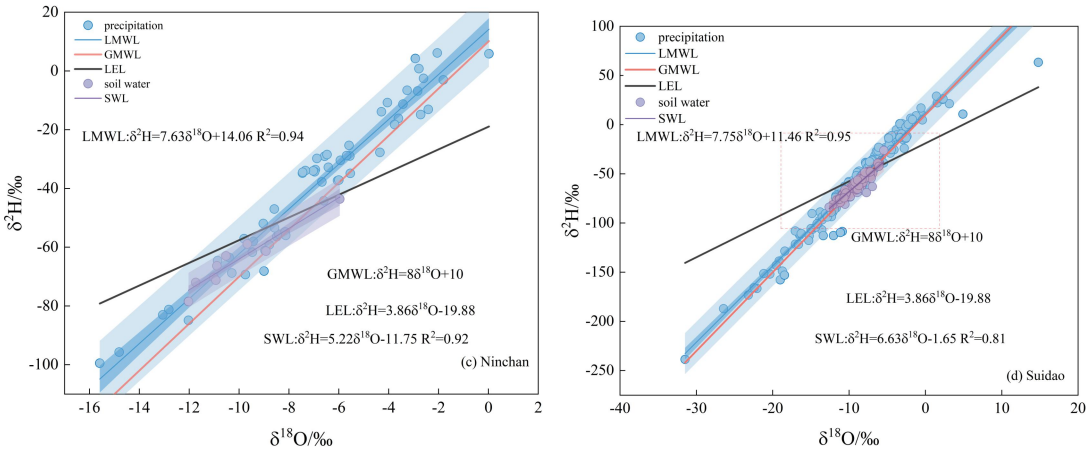

Figure 2 (a) Hydrogen and oxygen stable isotope linkages, (b) Precipitation and oxygen isotope changes in different water bodies.

Unsaturated water vapor leads to non-equilibrium fractionation during the process of precipitation, with an average d-excess value of 16.58‰ throughout the growing season (Figure 3, a). In May and September, due to higher relative humidity compared to other periods, the evaporation rate of water vapor is faster. The deuterium values show slow fluctuations from June to August, with significant fluctuations starting from mid-August, indicating that local evaporation is gradually enhanced over time due to the influence of temperature and relative humidity, leading to increased non-equilibrium evaporation. The average lc-excess value of precipitation in the lower layer of forest distribution is -8.18‰, while the average lc-excess value of precipitation in the middle, upper-middle, and canopy layers is close to 0. This is because the fractionation effect of evaporation is more pronounced at lower elevations. At higher elevations, influenced by rainfall and snowmelt, the soil moisture content in all soil layers is above 30% (Figure 3, b). Towards the end of the growing season, as temperatures decrease, tree leaves fall to the forest floor, forming a litter layer that retains moisture in the soil.

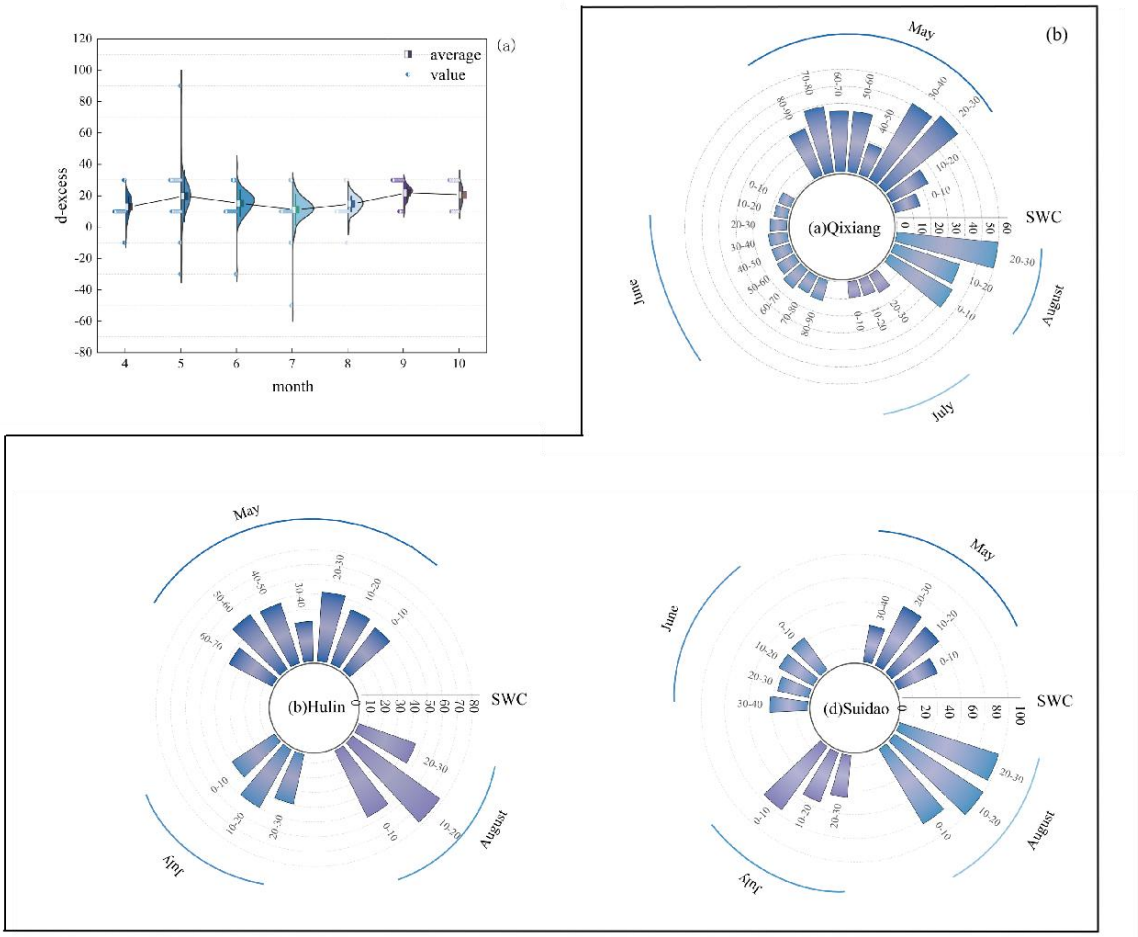

Figure 3 (a) Variation in soil water content, (b) Comparison between atmospheric water vapour oxygen isotopes and d-excess

4.2 Soil evaporation, plant transpiration and ecosystem evapotranspiration

Table 3 Evaporation and transpiration at different altitudes during the growing season

Site	Type	April	May	June	July	August	September	October
Qixiang	δ_T	2.22	-5.87	-4.59	-0.72	-1.72	-1.78	-2.26
	δ_E	-30.32	-28.68	-27.33	-29.12	-28.68	-26.32	-27.27
	δ_{ET}	-20.19	-20.05	-11.63	-9.87	-13.56	-15.85	-21.56
Hulin	δ_T	-5.34	-3.58	-4.13	-0.34	-2.35	-4.25	-1.97
	δ_E	-29.68	-27.28	-25.8	-27.75	-24.56	-25.21	-27.88
	δ_{ET}	-21.59	-22.36	-8.93	-10.17	-11.57	-18.8	/

Ninchan	δ_T	/	-3.45	-1.98	-1.05	-6.68	/	/
	δ_E	/	-20.57	-26.31	-29.08	-18.22	-18.15	-18.22
	δ_{ET}	/	/	-12.46	-7.57	/	/	/
Suidao	δ_T	/	-8.45	-6.98	-6.05	-6.68	/	/
	δ_E	-29.79	-27.32	-27.91	-23.83	-28.78	-25.8	-28.06
	δ_{ET}	-24.31	-16.14	-15.19	-10.07	-18.05	-23.02	-18.65

The Keeling plot method was used to analyze the stable isotope composition of ecosystem evapotranspiration (Figure 4). Its principle involves linearly fitting the water vapor concentration in the ecosystem boundary layer against the oxygen isotope composition, with the intercept on the y-axis representing the stable isotope value of δ_{ET}. The results indicate that at different heights within the distribution of deciduous trees, the average δ_{ET} value is -22.59‰. Throughout the entire growing season, δ_{ET} does not consistently decrease with increasing elevation. Specifically, near the treeline, there are higher stable isotope values, but in the middle and upper layers of the forest, there is a minimal value, indicating lower and less stable isotopic fractionation in that layer. At an elevation of 3448m, as the number of deciduous trees decreases and shrubs become dominant, the δ_{ET} value is -21.81‰(Table 3). We found that the stable isotope δ_E of soil evaporation at depths of 0-10cm is more enriched at lower elevations, particularly in April and May when the isotopic enrichment is more pronounced. From June to August, due to a significant increase in vegetation coverage, soil evaporation intensity decreases. In the early stage of the growing season, when leaves have not fully developed, the stable isotope composition of the xylem exhibits a relatively depleted characteristic. In July and August, when leaves are fully expanded, temperatures rise, and the rainy season in mountainous areas commences, transpiration becomes more intense.

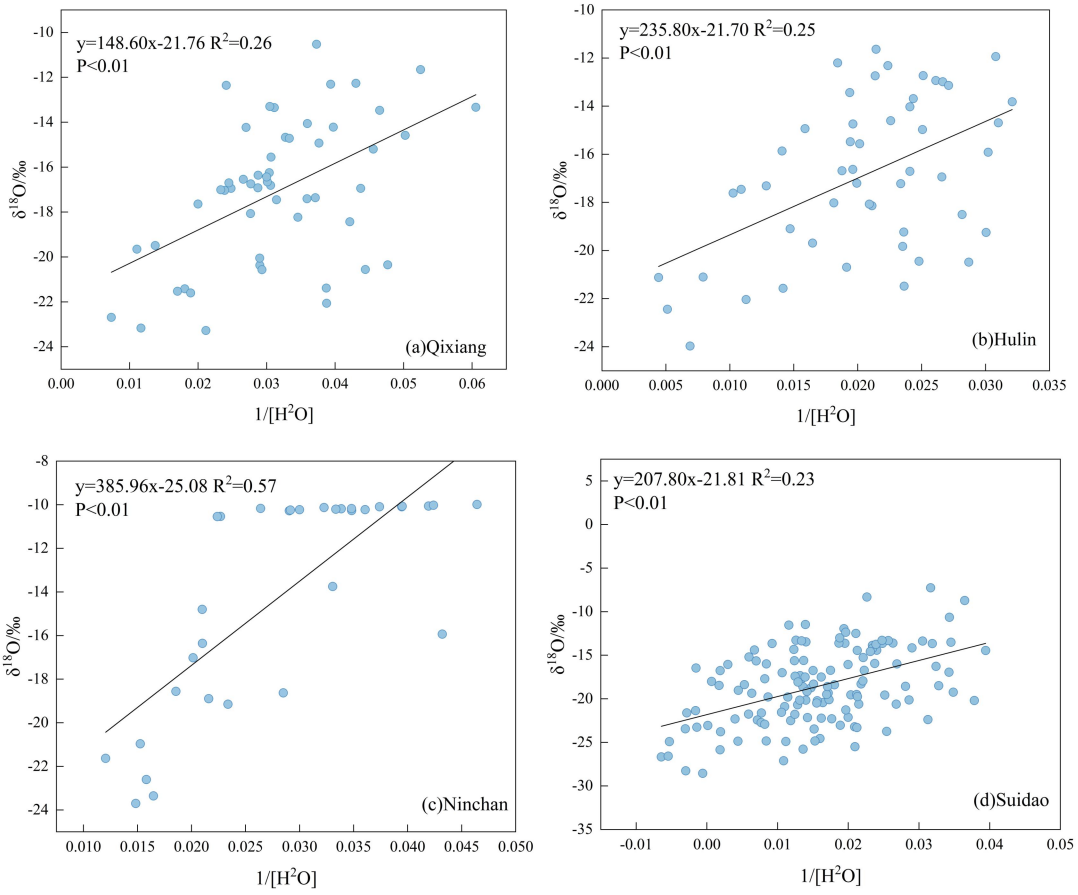

Figure 4 Each sampling point is fitted with a trend line based on the Keeling plot method

4.3 T/ET assessment of Qinghai spruce forest ecosystem in different months

We found that the canopy closure of deciduous trees significantly influences the evapotranspiration of the entire ecosystem (Figure 5). In April and May, as temperatures rise, surface vegetation exhibits weaker growth, resulting in a higher proportion of soil evaporation within the ecosystem, while transpiration by vegetation remains relatively low. During the rainy season in June to August, vegetation experiences vigorous growth, and transpiration reaches its peak in July. In September and October, soil evaporation becomes more dominant as temperatures, relative humidity, and rainfall gradually decrease, and deciduous tree leaves become wilted. At lower elevations, the T/ET ratio fluctuates between 0.20 and 0.70 in a distinct pattern, while above the treeline, transpiration ratios fluctuate between 0.20 and 0.80

in a similar pattern. Overall, summer is characterized as the peak season for transpiration, with a minimal contribution from soil evaporation.

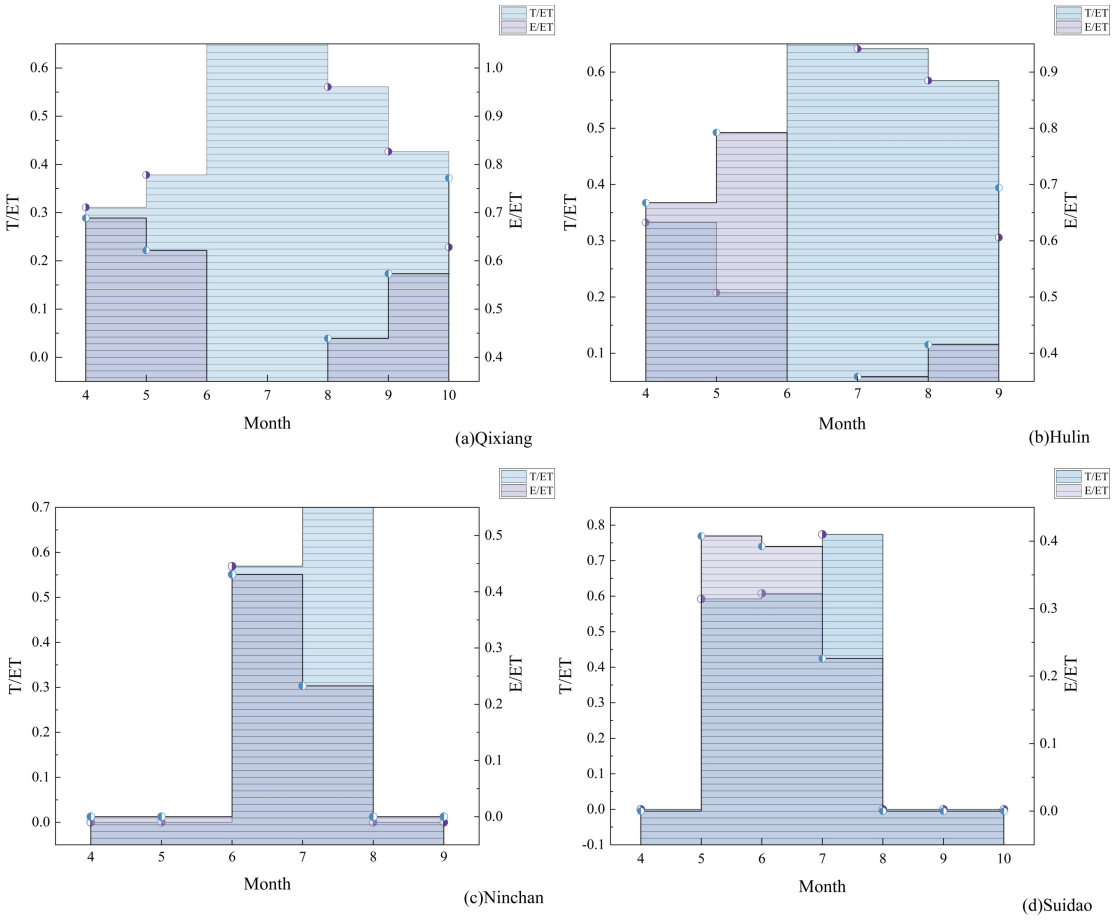

Figure 5 The proportion of soil evaporation and vegetation transpiration in evapotranspiration of ecosystem(0 represents missing data)

5. Discussions

5.1 Hydrological effects of changes in evapotranspiration

5.1.1 Impact on surface runoff

Comparing the differences of monthly potential evapotranspiration, surface evapotranspiration and precipitation in spruce forests (Table 4), the results clearly showed that rainfall fluctuated between 0-16mm, and the maximum rainfall was 15.7 mm in April, while the minimum value of surface evapotranspiration is 41.8 mm and the minimum value of potential evapotranspiration is 44.1mm. The difference

between ET_P and ET shows that there is no effective water accumulation in all months. From this, an important conclusion can be drawn: due to the late arrival of the rainy season in mountainous areas and the uneven distribution of rainfall across different altitudinal gradients, surface runoff can not be collected in this area, which also proves that afforestation in this area will further enhance evapotranspiration, posing a threat to water distribution and utilisation.

Table 4 Month-by-month comparison of potential evapotranspiration, surface evapotranspiration and rainfall

Variable \ Month	4	5	6	7	8	9	10
ET_p/mm	76.6	87.6	106.5	128.3	118.1	80.0	44.1
ET/mm	51.5	66.3	93.3	108.9	110.7	81.2	41.8
P/mm	15.7	8.8	0	13.2	13.3	11.2	13.6

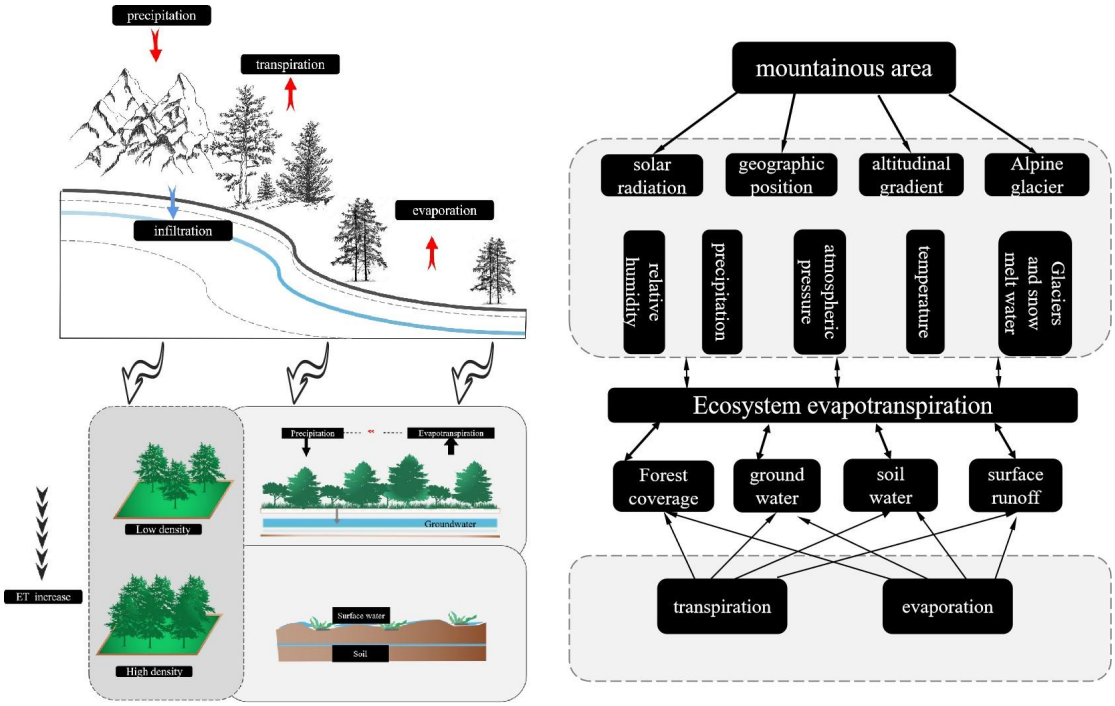

Figure 6 Conceptual model of the hydrological effects of changes in evapotranspiration

Some studies suggested that reducing forest density will result in less ET in seasonally dry forests. That reduced ET can be converted into increased groundwater and runoff to supply downstream social water (Wyatt, O'Donnell, & Springer, 2015). It has also been claimed that in some cases, the transient increase in water availability through reduced forest density can actually contribute to subsequent increases in vegetation cover and ultimately reduce runoff (Tague et al., 2019). By assessing the hydrological effects of afforestation through the water cycle in the Asia-Pacific region, it was found that in 7 of the 15 water-deficient areas, positive effects such as increased yield, precipitation, soil moisture and reduced drought risk were achieved through afforestation, and it was confirmed that the water-water cycle had a strong impact and evapotranspiration was increased (Teo et al., 2021). The water vapour content produced by forest transpiration is much higher than that lost by soil surface evaporation, most of the precipitation is intercepted and infiltrated by surface vegetation, and part of the soil water involved in infiltration is absorbed by the root zone of vegetation(Figure 6). Because of plants' high interception and evaporation ability and the absorption of groundwater by root zone, the proportion of transpiration was significantly higher than that of evaporation(Su et al., 2014). In this case, the groundwater amount decreases gradually with the T value increase. Under the influence of precipitation loss mainly due to plant transpiration, groundwater yield in this region decreases greatly, and has no significant contribution to the downstream water revenue.

5.1.2 Contribution to recirculating water vapour in precipitation

Our previous study in the eastern section of the Qilian Mountains (Zhang et al., 2021) indicated that above an altitude of 2100m, air masses gather from the northern foothills and move along the valley from low to high elevations. From June to August, the atmospheric circulation is influenced by westerlies, southeast monsoons, and plateau monsoons, while from September to October, the westerlies are the dominant factor. Therefore, we selected the Xiying station at an altitude of 2097m as our upwind site. The δ_{pv} values showed depletion in April and October, gradually

enriching from June to August. The maximum δ^2H value was -76.02‰ (Table 5), and the minimum was -184.93‰, while the maximum $\delta^{18}O$ value was -11.89‰, and the minimum was -26.38‰. Above 2700 meters, there is a gradual decrease in precipitation vapor with increasing altitude. The δ_{ev} values exhibited significant fluctuations throughout each month, with different patterns at different locations. At 2721m, the δ_{ev} range varied between -172.3‰ and 96.39‰. From the forest's lower layer to the upper layer, the isotopic composition of the advected moisture from the valley gradually diminished, resulting in decreasing values of δ_{adv}.

Table 5 Isotopic Composition of Precipitation Vapor, Surface Evaporation Vapor, and Vegetation Transpiration Vapor at Different Months and Altitudes

Month	Type	isotope	April	May	June	July	August	September	October
Qixiang	δpv	δ^2H/‰	-141.95	-123.83	-99.87	-115.99	-128.34	-120.9	-152.43
		$\delta^{18}O$/‰	-19.27	-16.58	-14.04	-15.91	-18.6	-17.22	-22.34
	δev	δ^2H/‰	-	-125.69	-123.69	-117.98	-134.57	-	-
		$\delta^{18}O$/‰	-	-30.21	-29.56	-28.62	-31.19	-	-
	δtr	δ^2H/‰	-39.9	-29.32	-46.19	-49.58	-45.15	-42.66	-44.64
		$\delta^{18}O$/‰	2.22	-5.87	-4.59	-0.72	-1.72	-1.78	-2.26
	δadv	δ^2H/‰	-145.57	-83.25	-81.12	-92	-109.62	-100.53	-122.62
		$\delta^{18}O$/‰	-20.24	-11.93	-10.73	-12.06	-15.31	-13.46	-18.16
Hulin	δpv	δ^2H/‰	-129.93	-123.29	-98.68	-113.98	-124.16	-118.52	-164.82
		$\delta^{18}O$/‰	-17.54	-16.62	-13.18	-15.48	-17.33	-17.88	-22.46
	δev	δ^2H/‰	-114.24	-117.01	-107.75	-123.44	-106.92	-96.39	-172.3
		$\delta^{18}O$/‰	-14.77	-16.35	-15.03	-16.7	-14.53	-12.78	-24.82
	δtr	δ^2H/‰	-24.12	-39.62	-35.97	-26.44	-35.85	-38.39	-40.53
		$\delta^{18}O$/‰	-5.34	-3.58	-4.13	-0.34	-2.35	-4.25	-1.97
	δadv	δ^2H/‰	-112.79	-115.67	-106.61	-122.19	-106.49	-95.7	-170.54
		$\delta^{18}O$/‰	-14.59	-16.15	-14.88	-16.54	-14.46	-12.69	-24.57
Ninchan	δpv	δ^2H/‰	-	-76.02	-139.21	-135.74	-129.96	-113.71	-184.93
		$\delta^{18}O$/‰	-	-11.89	-19.87	-18.7	-17.91	-16.77	-26.38
	δev	δ^2H/‰	-	-83.76	-81.42	-92.42	-110.24	-101.11	-123.42
		$\delta^{18}O$/‰	-	-12.01	-10.76	-12.09	-15.37	-13.49	-18.27
	δtr	δ^2H/‰	-	-25.58	-46.77	-37.77	-43.66	-	-
		$\delta^{18}O$/‰	-	-3.45	-1.98	-1.05	-6.68	-	-
	δadv	δ^2H/‰	-162.36	-113.49	-111.45	-106.16	-122.12	-114.67	-141.33
		$\delta^{18}O$/‰	-22.73	-15.94	-15.28	-14.46	-16.96	-16.58	-20.42
Suidao	δpv	δ^2H/‰	-167.86	-128.08	-124.95	-117.32	-137.73	-130.44	-155.52

δev	$\delta^{18}O$/‰	-22.9	-18.02	-17.28	-16.04	-19.09	-18.64	-21.59
	$\delta^{2}H$/‰	-164.16	-114.52	-112.37	-106.9	-122.96	-115.47	-142.85
δtr	$\delta^{18}O$/‰	-22.98	-16.07	-15.41	-14.56	-17.08	-16.69	-20.64
	$\delta^{2}H$/‰	-	-25.58	-46.77	-37.77	-43.66	-	-
δadv	$\delta^{18}O$/‰	-	-8.45	-6.98	-6.05	-6.68	-	-
	$\delta^{2}H$/‰	-162.38	-113.51	-111.47	-106.18	-122.14	-114.69	-141.36
	$\delta^{18}O$/‰	-22.73	-15.94	-15.28	-14.47	-16.97	-16.58	-20.42

In July, the ratio of vegetation transpiration to precipitation vapor is significantly higher compared to other months. The temperatures in the lower layers of the forest are relatively high, and the middle to upper layers are densely populated with spruce, resulting in a higher f_{tr} (transpiration ratio) throughout the entire growing season. Both the early and late stages of the growing season exhibit noticeably higher f_{ev} (evaporation ratio) compared to other months, with the middle and upper parts of the forest having a higher proportion of evaporated vapor. The average f_{adv} (advected vapor ratio) is 72%, with contributions exceeding 70% for all months except June and July (Figure 7).

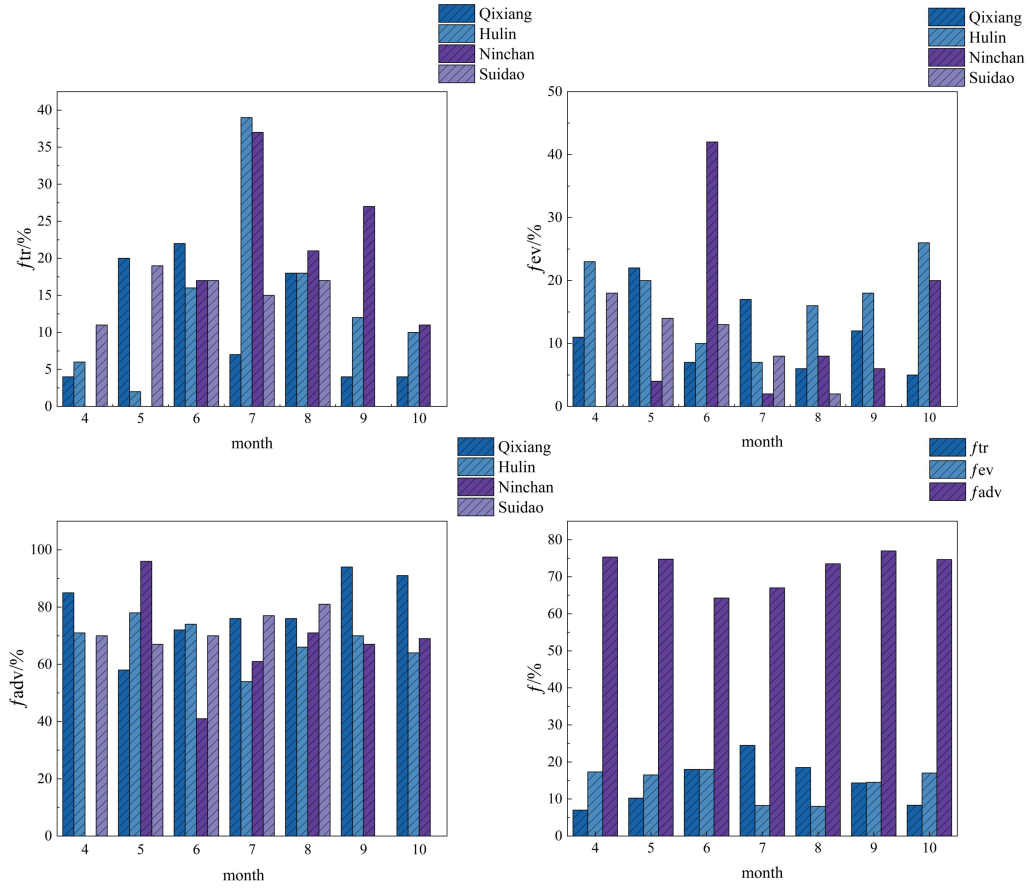

Figure 7 Comparison of f_{adv} (advective water vapour contribution), f_{ev} (surface evaporation water vapour contribution) and f_{tr} (plant transpiration water vapour contribution) for each of period

5.2 Uncertainty analysis

A higher sample size can reduce the margin of error. Therefore, we utilized isotopic data from four sites over a two-year period to evaluate the model. We used 404 xylem samples to calculate the contribution ratio of transpiration to ecosystem evapotranspiration. We examined the uncertainty of the model evaluation. When analyzing the evaporation characteristics in a semi-arid natural environment using the Craig-Gordon isotopic model, we first eliminated the influence of solar radiation and other meteorological variables on the calculation results. We focused on temperature, relative humidity, water vapor, and the initial isotopic values of water bodies. Particularly in semi-arid environments, the

variations in temperature and relative humidity are crucial (Hernández-Pérez et al., 2020). To verify the calculation results, we found a strong correlation between the isotopes of soil evaporation and relative humidity, as demonstrated by the fitting of δ_E against relative humidity and temperature. This also indicates the reliability of the results obtained through the Craig-Gordon isotopic model. We employed the Keeling plot method to calculate δ_{ET}, which is based on isotopic mass balance and a two-endmember mixing model. This method assumes that the isotopic composition of the background atmosphere and source remains constant, with a very low probability of isotopic spatial variation (Good et al., 2012; Kool et al., 2014). Due to the higher reliability of oxygen isotopes compared to hydrogen isotopes (Han et al., 2022; Kale et al., 2022), we solely used oxygen isotopes to calculate the T/ET values. The results indicate that transpiration significantly outweighs evaporation during July and August, which aligns with previous research findings (Zhu et al., 2022). The correlation between T/ET and soil moisture content suggests that soil moisture is a crucial factor driving the variations in transpiration and evaporation ratios. Additionally, the estimation of isotopic composition of advected water vapor from the upwind sites contributes to increased uncertainty. In our study area, the sites are predominantly influenced by valley winds, with water vapor moving from the valley bottom to higher altitudes. Therefore, we selected lower elevation areas in the valley bottom as the source region for advected water vapor (Zhang et al., 2021).

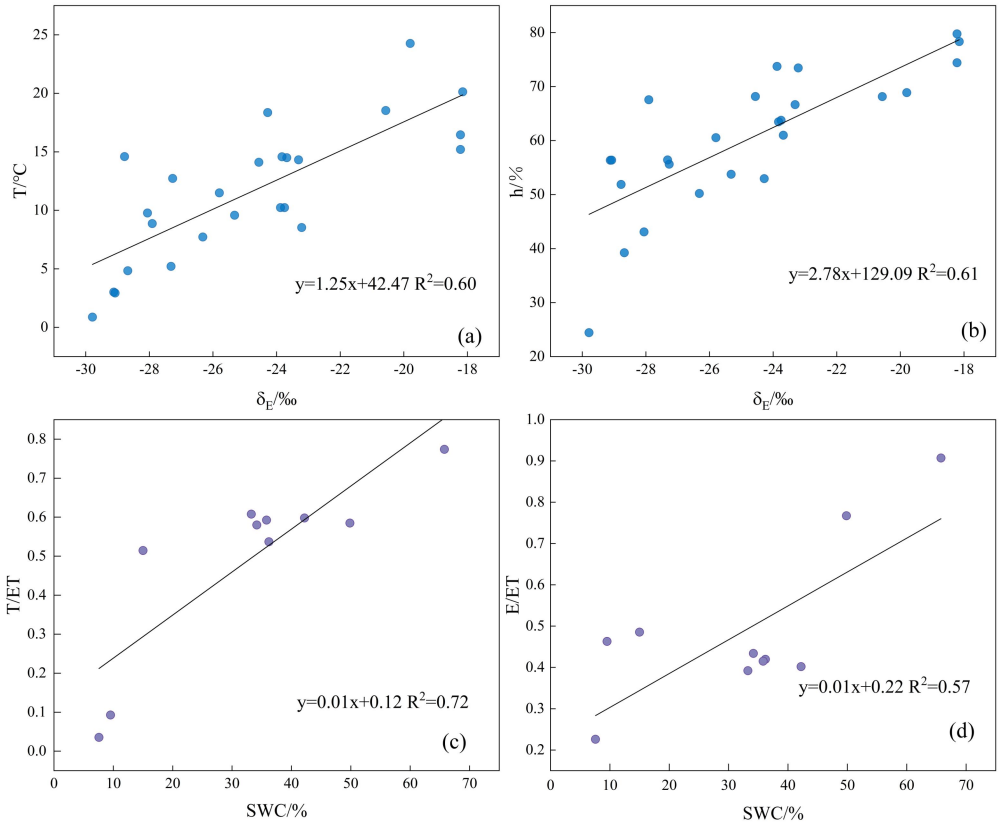

Figure 8 Correlation analysis of factors affecting uncertainty in impact assessment

6 Conclusions

This study utilizes isotopic data obtained from field observations during 2018-2019, combined with model simulations, to elucidate the mechanisms of evapotranspiration in the Qilian Mountains' spruce forests. The aim is to clarify the connection between evapotranspiration and local water cycling, as well as its hydrological effects. Isotopic methods were employed to assess T/ET (transpiration over evapotranspiration). The results indicate that July and August are the peak transpiration seasons for spruce, as they rely on favorable rainfall and thermal conditions. Both evaporation and transpiration are more intense during these months compared to other months, suggesting that transpiration by spruce trees is more significant than soil evaporation. Further quantification of the respective contributions of plant transpiration and soil evaporation to evapotranspiration reveals an average T/ET value of 0.57 during the study period, with a maximum value of 0.77 in July. Thus, it can be concluded that transpiration

by forest trees constitutes the main component of evapotranspiration in the Qinghai spruce forest ecosystem. Analyzing the hydrological effects of spruce forest evapotranspiration, it is found that the evapotranspiration amount in each month is at least three times greater than the precipitation. Therefore, surface runoff formation in this area is challenging to rely on due to the significant influence of transpiration and evaporation. Comparing the contribution ratios of atmospheric water vapor from precipitation during spring, summer, and autumn, the results demonstrate that the period from June to August serves as the peak transpiration season for spruce forests, with plant transpiration accounting for as much as 25% of the total atmospheric water vapor, while surface evaporation contributes only 18%. In the context of global warming, drought and water scarcity, as well as climate changes dominated by relative humidity, have altered the ecological communities, ecosystem functions, ecosystem services, and land-climate interactions of spruce forests. Therefore, it is crucial to understand that the depletion of rainfall in this forest belt through evapotranspiration is vital for local water resource allocation and ecological conservation.

Acknowledgements

This research was financially supported by the National Natural Science Foundation of China (41867030, 41971036). The authors much thank the colleagues in the Northwest Normal University for their help in fieldwork, laboratory analysis, data processing.

Data availability statement

The data that support the findings of this study are available on request from the corresponding author, stable isotope data are not publicly available due to privacy or ethical restrictions. Potential evapotranspiration and surface evapotranspiration data are available from the National Tibetan Plateau Scientific Data Centre(TPDC).

Competing Interests

We undersigned declare that this manuscript entitled “Hydrological effects of evapotranspiration in the Qilian Mountains forest belt” is original, has not been published before and is not currently being considered for publication elsewhere.

The authors declare that they have no known competing financial interests or personal relationships that could have appeared to influence the work reported in this paper.

References

Anderegg W R L, Kane J M, Anderegg L D L. Consequences of widespread tree mortality triggered by drought and temperature stress[J]. Nature climate change, 2013, 3(1): 30-36.

Aron P G, Poulsen C J, Fiorella R P, et al. An isotopic approach to partition evapotranspiration in a mixed deciduous forest[J]. Ecohydrology, 2020, 13(6): e2229.

Ault T R. On the essentials of drought in a changing climate[J]. Science, 2020, 368(6488): 256-260.

Brubaker K L, Entekhabi D, Eagleson P S. Estimation of continental precipitation recycling[J]. Journal of Climate, 1993, 6(6): 1077-1089.

Chang Y, Ding Y, Zhang S, et al. Dynamics and environmental controls of evapotranspiration for typical alpine meadow in the northeastern Tibetan Plateau[J]. Journal of Hydrology, 2022, 612: 128282.

Chen H, Zhu G, Shang S, et al. Uncertainties in partitioning evapotranspiration by two remote sensing-based models[J]. Journal of Hydrology, 2022, 604: 127223.

Craig H, Gordon L I. Deuterium and oxygen 18 variations in the ocean and the marine atmosphere[J]. 1965.

Cui Y, Jia L, Fan W. Estimation of actual evapotranspiration and its components in an irrigated area by integrating the Shuttleworth-Wallace and surface temperature-vegetation index schemes using the particle swarm optimization algorithm[J]. Agricultural and Forest Meteorology, 2021, 307: 108488.

Díaz S, Kattge J, Cornelissen J H C, et al. The global spectrum of plant form and function[J]. Nature, 2016, 529(7585): 167-171.

Ding, Y.X., & Peng, S.Z. (2020). Spatiotemporal trends and attribution of drought across China from 1901–2100. Sustainability, 12(2), 477.

Ding, Y.X., Peng, S.Z. (2021). Spatiotemporal change and attribution of potential evapotranspiration over China from 1901 to 2100. Theoretical and Applied Climatology. https://doi.org/10.1007/s00704-021-03625-w.

Eisenhauer N, Weigelt A. Ecosystem effects of environmental extremes[J]. Science, 2021, 374(6574): 1442-1443.

Gao, C. J. (2018). Regional differences in land-atmosphere coupling and possible impacts of soil moisture over Eastern China. Nanjing University of Information Science & Technology (In Chinese).

Gibson J J, Reid R. Stable isotope fingerprint of open-water evaporation losses and effective drainage area fluctuations in a subarctic shield watershed[J]. Journal of Hydrology, 2010, 381(1-2): 142-150.

Gibson J J, Reid R. Water balance along a chain of tundra lakes: A 20-year isotopic perspective[J]. Journal of Hydrology, 2014, 519: 2148-2164.

Good S P, Soderberg K, Wang L, et al. Uncertainties in the assessment of the isotopic composition of surface fluxes: A direct comparison of techniques using laser-based water vapor isotope analyzers[J]. Journal of Geophysical Research: Atmospheres, 2012, 117(D15).

Goodwell A E, Kumar P, Fellows A W, et al. Dynamic process connectivity explains ecohydrologic responses to rainfall pulses and drought[J]. Proceedings of the

National Academy of Sciences, 2018, 115(37): E8604-E8613.

Han J, Tian L, Cai Z, et al. Season-specific evapotranspiration partitioning using dual water isotopes in a Pinus yunnanensis ecosystem, southwest China[J]. Journal of Hydrology, 2022, 608: 127672.

Hernández-Pérez E, Levresse G, Carrera-Hernández J, et al. Short term evaporation estimation in a natural semiarid environment: New perspective of the Craig–Gordon isotopic model[J]. Journal of Hydrology, 2020, 587: 124926.

Horita J, Wesolowski D J. Liquid-vapor fractionation of oxygen and hydrogen isotopes of water from the freezing to the critical temperature[J]. Geochimica et Cosmochimica Acta, 1994, 58(16): 3425-3437.

Kale Celik S, Madenoglu S, Turker U. Partitioning evapotranspiration of winter wheat based on oxygen isotope approach under different irrigation regimes[J]. Irrigation and Drainage, 2022, 71(4): 882-896.

Keeling C D. The concentration and isotopic abundances of atmospheric carbon dioxide in rural areas[J]. Geochimica et cosmochimica acta, 1958, 13(4): 322-334.

Kong Y, Pang Z, Froehlich K. Quantifying recycled moisture fraction in precipitation of an arid region using deuterium excess[J]. Tellus B: Chemical and Physical Meteorology, 2013, 65(1): 19251.

Kool D, Agam N, Lazarovitch N, et al. A review of approaches for evapotranspiration partitioning[J]. Agricultural and forest meteorology, 2014, 184: 56-70.

Li Q, Ye A, Zhang Y, et al. The peer-to-peer type propagation from meteorological drought to soil moisture drought occurs in areas with strong land-atmosphere interaction[J]. Water Resources Research, e2022WR032846.

Li X, Liang S, Yuan W, et al. Estimation of evapotranspiration over the terrestrial ecosystems in China[J]. Ecohydrology, 2014, 7(1): 139-149.

Liu Y, Lian J, Luo Z, et al. Spatiotemporal variations in evapotranspiration and transpiration fraction following changes in climate and vegetation in a karst basin of

southwest China[J]. Journal of Hydrology, 2022, 612: 128216.

Liu Y, Zhuang Q, Miralles D, et al. Evapotranspiration in Northern Eurasia: Impact of forcing uncertainties on terrestrial ecosystem model estimates[J]. Journal of Geophysical Research: Atmospheres, 2015, 120(7): 2647-2660.

Maxwell R M, Condon L E. Connections between groundwater flow and transpiration Partitioning [J]. Science, 2016, 353(6297): 377-380.

Peng W L, Zhao L J, Xie C, et al. Et segmentation of Picea Qinghai forest ecosystem in the upper reaches of Heihe River [J]. Journal of Glaciology and Geocryology, 2020, 42(2): 629-640.

Peng, S. (2022). 1 km monthly potential evapotranspiration dataset in China (1990-2021). National Tibetan Plateau Data Center, 2022. DOI: 10.11866/db.loess.2021.001.

Peng, S.Z., Ding, Y.X., Liu, W.Z., & Li, Z. (2019). 1 km monthly temperature and precipitation dataset for China from 1901 to 2017. Earth System Science Data, 11, 1931–1946. https://doi.org/10.5194/essd-11-1931-2019.

Peng, S.Z., Ding, Y.X., Wen, Z.M., Chen, Y.M., Cao, Y., & Ren, J.Y. (2017). Spatiotemporal change and trend analysis of potential evapotranspiration over the Loess Plateau of China during 2011-2100. Agricultural and Forest Meteorology, 233, 183-194. https://doi.org/10.1016/j.agrformet.2016.11.129.

Raz-Yaseef N, Rotenberg E, Yakir D. Effects of spatial variations in soil evaporation caused by tree shading on water flux partitioning in a semiarid pine forest[J]. Agricultural and Forest Meteorology, 2010, 150(3): 454-462.

Rohatyn S, Yakir D, Rotenberg E, et al. Limited climate change mitigation potential through forestation of the vast dryland regions[J]. Science, 2022, 377(6613): 1436-1439.

Sang L, Zhu G, Xu Y, et al. Effects of Agricultural Large-And Medium-Sized Reservoirs on Hydrologic Processes in the Arid Shiyang River Basin, Northwest China[J]. Water Resources Research, 2023, 59(2): e2022WR033519.

681 Schlesinger W H, Jasechko S. Transpiration in the global water cycle[J]. Agricultural and
682 Forest Meteorology, 2014, 189: 115-117.

683 Skrzypek G, Mydłowski A, Dogramaci S, et al. Estimation of evaporative loss based on
684 the stable isotope composition of water using Hydrocalculator[J]. Journal of
685 Hydrology, 2015, 523: 781-789.

686 Su T, Lu Z Y, Zhou J, et al. Spatial distribution and seasonal variation characteristics of
687 global atmospheric moisture recycling[J]. 2014.

688 Sun X, Wilcox B P, Zou C B. Evapotranspiration Partitioning in dryland ecosystems: A
689 global meta-analysis of in situ studies[J]. Journal of Hydrology, 2019, 576: 123-136.

690 Tague CL, Moritz M, Hanan E. The changing water cycle: The eco-hydrologic impacts of
691 forest density reduction in Mediterranean (seasonally dry) regions. WIREs Water.
692 2019;e1350. https://doi.org/10.1002/wat2.1350

693 Talsma C J, Good S P, Jimenez C, et al. Partitioning of evapotranspiration in remote
694 sensing-based models[J]. Agricultural and Forest Meteorology, 2018, 260: 131-143.

695 Teo H C, Raghavan S V, He X, et al. Large-Scale Reforestation Can Increase Water Yield
696 and Reduce Drought Risk for Water-Insecure Regions in the Asia-Pacific[J].
697 Available at SSRN 3989861.

698 Wang L, Good S P, Caylor K K. Global synthesis of vegetation control on
699 evapotranspiration partitioning[J]. Geophysical Research Letters, 2014, 41(19):
700 6753-6757.

701 Wang P, Yamanaka T, Li X Y, et al. Partitioning evapotranspiration in a temperate
702 grassland ecosystem: Numerical modeling with isotopic tracers[J]. Agricultural and
703 Forest Meteorology, 2015, 208: 16-31.

704 Wang S, Wang L, Zhang M, et al. Quantifying moisture recycling of a leeward oasis in
705 arid central Asia using a Bayesian isotopic mixing model[J]. Journal of Hydrology,
706 2022, 613: 128459.

707 Wei Z, Lee X, Wen X, et al. Evapotranspiration partitioning for three agroecosystems

with contrasting moisture conditions: a comparison of an isotope method and a two-source model calculation[J]. Agricultural and Forest Meteorology, 2018, 252: 296-310.

Wershaw, R.L., Friedman, I., Heller, S.J., Frank, P.A., 1966. Hydrogen isotope fractionation of water passing through trees. In: Hobson, G.D. (Ed.), Advances in OrganicGeochemistry. Pergamon Press, New York, pp. 55–67.

Wyatt, C. J. W., O'Donnell, F. C., & Springer, A. E. (2015). Semi-Arid Aquifer Responses to Forest Restoration Treatments and Climate Change.Groundwater, 53(2), 207–216.

Yao Y., Liang S., Li X., Chen J., Liu S., et al. Improving global terrestrial evapotranspiration estimation using support vector machine by integrating three process-based algorithms. Agricultural and Forest Meteorology 2017, 242, 55-74. DOI: 10.1016/j.agrformet.2017.04.011.

Yao, Y., Liu, S., Shang, K. (2020). Daily MODIS-based Land Surface Evapotranspiration Dataset of 2019 in Qilian Mountain Area (ETHi-merge V1.0). National Tibetan Plateau Data Center, 2020. DOI: 10.11888/Meteoro.tpdc.270407.

Yepez E A, Huxman T E, Ignace D D, et al. Dynamics of transpiration and evaporation following a moisture pulse in semiarid grassland: A chamber-based isotope method for partitioning flux components[J]. Agricultural and Forest Meteorology, 2005, 132(3-4): 359-376.

Yong L, Zhu G, Wan Q, et al. The soil water evaporation process from mountains based on the stable isotope composition in a headwater basin and northwest China[J]. Water, 2020, 12(10): 2711.

Zhang M, Wei X. Deforestation, forestation, and water supply[J]. Science, 2021, 371(6533): 990-991.

Zhang R, Xu X, Liu M, et al. Comparing evapotranspiration characteristics and environmental controls for three agroforestry ecosystems in a subtropical humid karst area[J]. Journal of hydrology, 2018, 563: 1042-1050.

735 Zhang Y, Gentine P, Luo X, et al. Increasing sensitivity of dryland vegetation greenness
736 to precipitation due to rising atmospheric CO^2[J]. Nature communications, 2022,
737 13(1): 1-9.

738 Zhang Z, Zhu G, Pan H, et al. Quantifying recycled moisture in precipitation in Qilian
739 Mountains[J]. Sustainability, 2021, 13(23): 12943.

740 Zhu G, Guo H, Qin D, et al. Contribution of recycled moisture to precipitation in the
741 monsoon marginal zone: Estimate based on stable isotope data[J]. Journal of
742 Hydrology, 2019, 569: 423-435.

743 Zhu G, Liu Y, Shi P, et al. Stable water isotope monitoring network of different water
744 bodies in Shiyang River basin, a typical arid river in China[J]. Earth System Science
745 Data, 2022, 14(8): 3773-3789.

746 Zhu G, Wang L, Liu Y, et al. Snow-melt water: An important water source for Picea
747 crassifolia in Qilian Mountains[J]. Journal of Hydrology, 2022, 613: 128441.

748